



**THE SOLUTION OF COMBINED  
CONVECTION AND RADIATION  
HEAT TRANSFER FROM LONGITUDINAL FINS  
OF ARBITRARY CROSS-SECTION**

**Percy B. Carter, Jr.**

**ARO, Inc.**

**April 1969**

This document has been approved for public release  
and sale; its distribution is unlimited.

**ENGINEERING SUPPORT FACILITY  
ARNOLD ENGINEERING DEVELOPMENT CENTER  
AIR FORCE SYSTEMS COMMAND  
ARNOLD AIR FORCE STATION, TENNESSEE**

PROPERTY OF U. S. AIR FORCE  
AEDC LIBRARY  
F40600-69-C-0001

# *NOTICES*

When U. S. Government drawings specifications, or other data are used for any purpose other than a definitely related Government procurement operation, the Government thereby incurs no responsibility nor any obligation whatsoever, and the fact that the Government may have formulated, furnished, or in any way supplied the said drawings, specifications, or other data, is not to be regarded by implication or otherwise, or in any manner licensing the holder or any other person or corporation, or conveying any rights or permission to manufacture, use, or sell any patented invention that may in any way be related thereto.

Qualified users may obtain copies of this report from the Defense Documentation Center.

References to named commercial products in this report are not to be considered in any sense as an endorsement of the product by the United States Air Force or the Government.

THE SOLUTION OF COMBINED  
CONVECTION AND RADIATION  
HEAT TRANSFER FROM LONGITUDINAL FINS  
OF ARBITRARY CROSS-SECTION

Percy B. Carter, Jr.  
ARO, Inc.

This document has been approved for public release  
and sale; its distribution is unlimited.

## FOREWORD

The work reported herein sponsored by the Arnold Engineering Development Center (AEDC), Air Force Systems Command (AFSC).

The results of research presented were obtained by ARO, Inc. (a subsidiary of Sverdrup & Parcel and Associates, Inc.), contract operator of the AEDC, AFSC, Arnold Air Force Station, Tennessee, under Contract F40600-69-C-0001. The research was conducted from May through November, 1968, under ARO Project No. TT8002, and the manuscript was submitted for publication on March 13, 1969.

The author expresses his sincere appreciation to Dr. Walter Frost, his advisor, for his patient and thoughtful counselling during the course of this study.

This manuscript was prepared in partial fulfillment of the requirements for the degree of master of science at The University of Tennessee Space Institute.

Publication of this report does not constitute Air Force approval of the report's findings or conclusions. It is published only for the exchange and stimulation of ideas.

Roy R. Croy, Jr.  
Colonel, USAF  
Director of Test

## ABSTRACT

The effects of combined radiative and convective heat transfer from arrays of longitudinal fins of arbitrary profile are analyzed subject to non-uniform surface emissivity and non-uniform surface film coefficients. Consideration is given to radiative interactions between adjacent fins and between fins and the base surface. Solution of the defining differential equation for fin temperature distribution is obtained through an iterative application of the B. G. Galerkin variational technique. Application of the method of solution is made to fins of parabolic, triangular, and inverse parabolic profile subject solely to the radiative mode of heat transfer. Effects in variations of the dimensionless radiation number,  $N_R$ , fin spacing,  $S$ , and fin surface emissivity,  $\epsilon$ , are investigated. Findings of the study reveal that for the pure radiative mode, fins can enhance the heat transfer between the base and the surroundings only for the case of low fin and base surface emissivity.

## TABLE OF CONTENTS

CHAPTER	PAGE
I. INTRODUCTION . . . . .	1
II. FORMULATION OF THE GENERAL PROBLEM . . . . .	5
Geometrical Considerations and Assumptions . . . . .	5
Derivation of the Basic Differential Equation . . . . .	7
Calculation of the Surface Radiation Terms . . . . .	8
Non-Dimensionalization of the Basic Differential Equation . . . . .	14
Transformation of the Non-Dimensional System . . . . .	17
III. SOLUTION OF THE DEFINING EQUATIONS BY THE B. G. GALERKIN METHOD . . . . .	19
Introduction of the Galerkin Method . . . . .	19
Formulation of the Algebraic System of Linear Equations . . . . .	21
Solution of the Algebraic System of Linear Equations . . . . .	26
IV. APPLICATION OF THE SOLUTION TECHNIQUE TO FINS OF SELECTED SHAPE . . . . .	28
Description of Selected Fin Shapes and Conditions of Analysis . . . . .	28
Description of Selected Mathematical Parameters . . . . .	29
V. PRESENTATION AND DISCUSSION OF RESULTS . . . . .	33

CHAPTER	PAGE
Temperature Distribution . . . . .	33
Fin Efficiency . . . . .	43
Apparent Emittance . . . . .	49
VI. CONCLUSIONS . . . . .	56
BIBLIOGRAPHY . . . . .	58
APPENDIXES . . . . .	61
A. NON-DIMENSIONALIZATION OF THE BASIC DIFFERENTIAL EQUATION . . . . .	62
B. BOUNDARY CONDITION CHECK OF ASSUMED GALERKIN FUNCTIONS . . . . .	69
C. COMPUTER PROGRAM LISTING . . . . .	72
VITA . . . . .	87

## LIST OF FIGURES

FIGURE	PAGE
1. Geometrical Conception of Arbitrary Fin Cluster . .	6
2. The Radiosity Concept . . . . .	10
3. Cavity Radiation . . . . .	11
4. Effects of $n$ on the Solution for Temperature Distribution . . . . .	30
5. Convergence of Successive Iterations . . . . .	32
6. Dimensionless Temperature Distribution in a Parabolic Fin . . . . .	34
7. Dimensionless Temperature Distribution in a Triangular Fin . . . . .	37
8. Dimensionless Temperature Distribution in an Inverse Parabolic Fin . . . . .	40
9. Parabolic Fin Efficiency . . . . .	45
10. Triangular Fin Efficiency . . . . .	46
11. Inverse Parabolic Fin Efficiency . . . . .	47
12. The Apparent Emittance of a Parabolic Fin Cluster .	50
13. The Apparent Emittance of a Triangular Fin Cluster . . . . .	51
14. The Apparent Emittance of an Inverse Parabolic Fin Cluster . . . . .	52
15. Apparent Emittance of Clusters of Fins of Selected Shapes . . . . .	54

## NOMENCLATURE

A	Area
a	Galerkin coefficients defined by Equation 21
B	Radiosity
F	Shape factor
f(X)	Mathematical function defined by Equation 16
G(i)	Mathematical function defined by Equations 26 and 30.
g(X)	Mathematical function defined by Equation 16
H	Incident radiation
h	Surface convective film coefficient (dimensional)
$\bar{h}$	Surface convective film coefficient (dimensionless)
I(k,i)	Mathematical function defined by Equations 26 and 30
J(i)	Mathematical function defined by Equations 26 and 30
K	Thermal conductivity (dimensional)
$\bar{K}$	Thermal conductivity (dimensionless)
L	Fin length
$N_R$	Radiation number, $\sigma T_o^4 L / K_c (T_o - T_{g\infty})$
$N_C$	Biot's number, $h_c L / K_c$
n	The number of terms appearing in the Galerkin solution
Q	Dimensionless heat flux

q	Dimensional heat flux
S	Dimensionless fin spacing
s	Dimensional fin spacing
T	Temperature
X	Non-dimensional distance measured along the fin
x	Dimensional distance measured along the fin
Y	Fin surface height
Z(k,i)	Matrix element defined by Equations 28 and 32
ZH(i)	Column matrix element defined by Equations 28 and 32
$\alpha$	Absorptivity
$\beta^*$	Boundary condition parameter, $h_c \bar{h}^*(1)/K_C K(1)$
$\chi_{ij}$	Matrix element defined by Equation 9
$\delta_{ij}$	Kronecker delta
$\epsilon$	Emissivity
$\epsilon_A$	Apparent emittance
$\eta$	Fin efficiency
$\Omega_{ij}$	Matrix element defined by Equation 8
$\Lambda_{ij}$	Matrix element defined by Equation 12
$\phi_i$	Galerkin function defined by Equation 21
$\psi$	Transformed non-dimensional temperature
$\rho$	Reflectivity
$\sigma$	Stefan-Boltzmann constant = $1.71 \times 10^{-9}$ Btu/Hr-Ft <sup>2</sup> -°R
$\theta$	Non-dimensional temperature defined by Equation 13

**Subscripts**

- C Indicates convection heat transfer related expression
- c Characteristic reference value
- R Indicates radiation heat transfer related expression
- g Property of ambient fluid
- $g_{\infty}$  Characteristic reference value of fluid in which the fin cluster is immersed
- o Value at fin base
- 1 Value on upper fin surface ( $Y > 0$ )
- 2 Value on lower fin surface ( $Y < 0$ )
- k,i Index of finite set of Galerkin functions
- i,j Index of surface elements in enclosure radiation analysis

**Superscripts**

- \* Indicates value at fin tip

## CHAPTER I

## INTRODUCTION

Heat transfer phenomena associated with convection from arrays of longitudinal fins has been the subject of many theoretical and experimental investigations since early in this century. Most early investigators (1, 2, 3)<sup>1</sup> limited their interest to single fins of simplified geometry and employed certain classical assumptions such as uniform convective film coefficients and negligible influence of the fin surface slope. In all cases the influence of radiation to the environment and to surrounding surfaces was neglected.

In 1951, Ghai (4) experimentally demonstrated that for certain fin configurations the convective film coefficients were larger near the tip than near the fin base. Ghai concluded that the classical assumption of uniform film coefficients was not, in general, valid.

Eraslan and Frost (5) have solved the problem of the longitudinal convection fin subject to non-uniform film coefficients. Their study indicates that fins previously considered as being optimum when analyzed assuming uniform film coefficients, did not necessarily remain so when the

---

<sup>1</sup>Numbers in parentheses refer to similarly numbered references in the bibliography.

effects of non-uniform film coefficients were considered. Eraslan and Frost applied a variational method due to B. G. Galerkin in their solution.

With the advent of the space age, the pure radiation fin became of significance. Several authors (6, 7) considered a single fin radiating to an isothermal environment where interactions were neglected. Eckert, Irvine, and Sparrow (8, 9), in 1960, published a series of papers which formulated the basic equations defining radiative interaction in arrays of longitudinal fins. Their problem considered radiative interactions of the fins with adjacent fins and with base surfaces. These authors, however, limited the application of their analysis to fairly simplified shapes in which radiative interaction from base surfaces could be ignored. Herring (10) extended the same problem to include specular reflecting surfaces.

In a later paper (11) Sparrow and Eckert applied the generalized equations to a configuration consisting of a longitudinal fin connecting two, isothermal cylindrical surfaces. They treated the surfaces as black and included all radiative interaction effects. An iterative Runge-Kutta technique was used to solve the governing integral differential equations. Sarabia (12), by application of an iterative finite difference technique, extended the work of Sparrow and Eckert to include grey surfaces.

Recently Frost and Eraslan (13) published a study of

radiation from arrays of longitudinal, rectangular profile fins in which the effects of mutual irradiation were considered. They solved the defining non-linear integro-differential equation through an iterative technique using the variational method of Galerkin. Their study indicated that interaction effects did indeed have an important influence on the equilibrium temperature distribution along the fin. Frost and Eraslan also concluded that the Galerkin method of solving the differential equations had a distinct computational advantage over the heretofore employed numerical methods.

The study of the combined effects of convection and radiation from single fins has also been the subject of recent investigations (14, 15). Frost and Eraslan (16) have extended the theory to arrays of longitudinal rectangular fins in which the effects of radiative interactions under the combined modes of radiation and convection heat transfer are considered. Their study indicated that the efficiency of fins under the combined modes of heat transfer was less than for the pure convection case.

The present analysis extends the work of Frost and Eraslan to cover longitudinal fins of arbitrary cross-section subject to the combined modes of heat transfer. The method of solution is formulated to include the effects of non-uniform surface film coefficients and surface emissivities and the effects of mutual irradiation. However,

because of the vast amount of data generated by an exhaustive study of this type of fin heat transfer phenomena, the results generated by the method of solution are reported only for a selected group of fin configurations subject solely to radiative heat transfer.

## CHAPTER II

## FORMULATION OF THE GENERAL PROBLEM

## I. GEOMETRICAL CONSIDERATIONS AND ASSUMPTIONS

A typical array of longitudinal fins of arbitrary cross-section projecting from a plane base surface is shown in Figure 1. The x-axis is chosen to run parallel to the axis of the fin and perpendicular to the base surface.

The analysis is predicated on the following assumptions:

1. Heat conduction along the fin is one-dimensional and occurs in the x-direction.
2. Each fin, while of arbitrary cross-section, possesses a geometry that is similar to all other fins in the array.
3. The fins are immersed in a non-participating radiation medium and have grey surfaces.
4. Fin surface geometry is defined as a function of the x-coordinate.
5. The gas medium temperatures are known functions of the x-coordinate.
6. Surface film coefficients, thermal conductivity, and surface emissivity of the fin are prescribed functions of the x-coordinate.

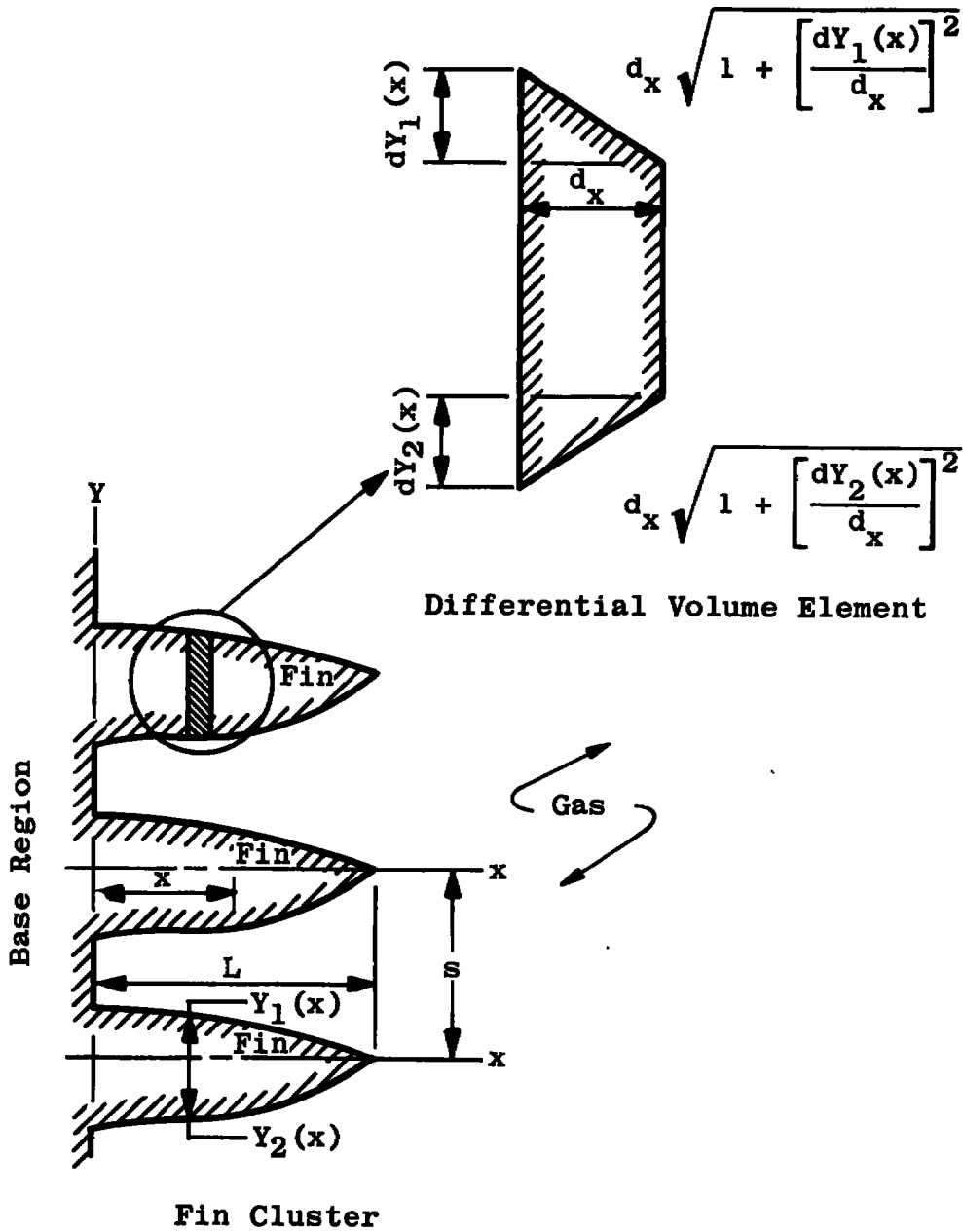


Figure 1. Geometrical conception of arbitrary fin cluster.

7. The heat transfer process occurs at a steady rate.
8. The base surface exists at a constant temperature,  $T_o$ .
9. The problem is formulated for a fin of unit depth.

## II. DERIVATION OF THE BASIC DIFFERENTIAL EQUATION

The differential equation of the phenomenon is formed in the classical manner by making an energy balance on a typical differential volume element as shown in Figure 1. The various modes of energy transport considered are internal conduction and radiative and convective transfer from the fin surface. Performing the energy balance produces the following form of the general equation:

$$\begin{aligned}
 & -K(x)A(x)\frac{dT(x)}{dx} + \left\{ K(x)A(x)\frac{dT(x)}{dx} + \frac{d\left[ K(x)A(x)\frac{dT(x)}{dx} dx \right]}{dx} \right\} \\
 & = h_1(x)A_1(x)[T(x) - T_{g1}(x)] + h_2(x)A_2(x)[T(x) - T_{g2}(x)] \\
 & + q_{R1}(x)A_1(x) + q_{R2}(x)A_2(x) \qquad (1)
 \end{aligned}$$

where  $K(x)$ ,  $h_1(x)$ , and  $h_2(x)$  represent the fin thermal conductivity and surface film coefficients of the corresponding

surfaces respectively. Expressing the area terms as functions of the fin geometry, simplifying, and collecting terms, leads to Equation 2. It should be noted that fin surface slopes,  $\sqrt{1 + (dY/dx)^2}$ , are included in Equation 2.

$$\begin{aligned}
 & K(x) [Y_1(x) - Y_2(x)] \frac{d^2 T(x)}{dx^2} + \left\{ K(x) \left[ \frac{dY_1(x)}{dx} - \frac{dY_2(x)}{dx} \right] \right. \\
 & \left. + [Y_1(x) - Y_2(x)] \frac{dK(x)}{dx} \right\} \frac{dT(x)}{dx} \\
 & - \left[ h_1(x) \sqrt{1 + \left( \frac{dY_1(x)}{dx} \right)^2} + h_2(x) \sqrt{1 + \left( \frac{dY_2(x)}{dx} \right)^2} \right] T(x) \\
 & = - \left[ h_1(x) \sqrt{1 + \left( \frac{dY_1(x)}{dx} \right)^2} T_{g1}(x) + h_2(x) \sqrt{1 + \left( \frac{dY_2(x)}{dx} \right)^2} \right. \\
 & \left. \cdot T_{g2}(x) \right] + q_{R1}(x) \sqrt{1 + \left( \frac{dY_1(x)}{dx} \right)^2} \\
 & + q_{R2}(x) \sqrt{1 + \left( \frac{dY_2(x)}{dx} \right)^2} \tag{2}
 \end{aligned}$$

Associated with Equation 2 are boundary conditions as follows:

1. At  $x = 0$ ;  $T(0) = T_0$ .
2. At  $x = L$ ;  $-K(L) \frac{dT(L)}{dx} = q_R^* + h^* [T(L) - T_g(L)]$ . (3)

### III. CALCULATION OF THE SURFACE RADIATION TERMS

A closer look will now be taken at the surface

radiation terms  $q_{R1}(x)$  and  $q_{R2}(x)$  which appear in Equations 1 and 2. The radiative energy flux emanating from the fin surfaces can be computed by treating the volume between the fins as a cavity and applying a method described by Sparrow and Cess (17) for analyzing radiation within enclosures.

The method of Sparrow and Cess assumes that the walls of the enclosure can be broken up into  $(k)$  isothermal grey, opaque, diffuse surfaces. The radiosity  $(B)$ , defined as the rate of energy per unit surface area streaming away from a given surface, is composed of two components; the emitted energy  $(\epsilon\sigma T^4)$ , and the reflected portion of the incident energy. The energy incident on unit area of surface  $(i)$  is denoted as  $H_i$ . Figure 2 illustrates the radiosity concept.

Working with total radiation properties, it can be shown that the reflectivity of any grey surface can be represented as  $\rho = (1 - \epsilon)$ , where  $\rho$  is the reflectivity and  $\epsilon$  is the emissivity. Hence, for a surface denoted with the subscript  $(i)$  the expression for radiosity becomes as indicated by Equation 4.

$$B_i = \epsilon_i \sigma T_i^4 + (1 - \epsilon_i) H_i \quad (4)$$

Figure 3 illustrates a typical surface configuration in the enclosure formed by adjacent longitudinal fins. The  $i$ 'th surface element is shown receiving radiation from other surface elements, from the base region, and from the gas

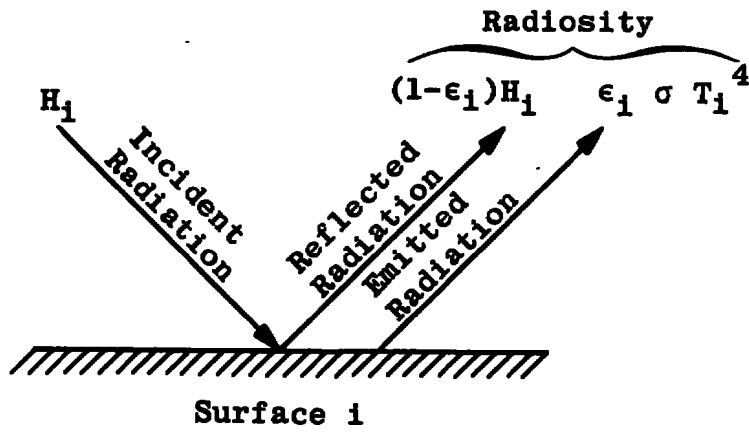


Figure 2. The radiosity concept.

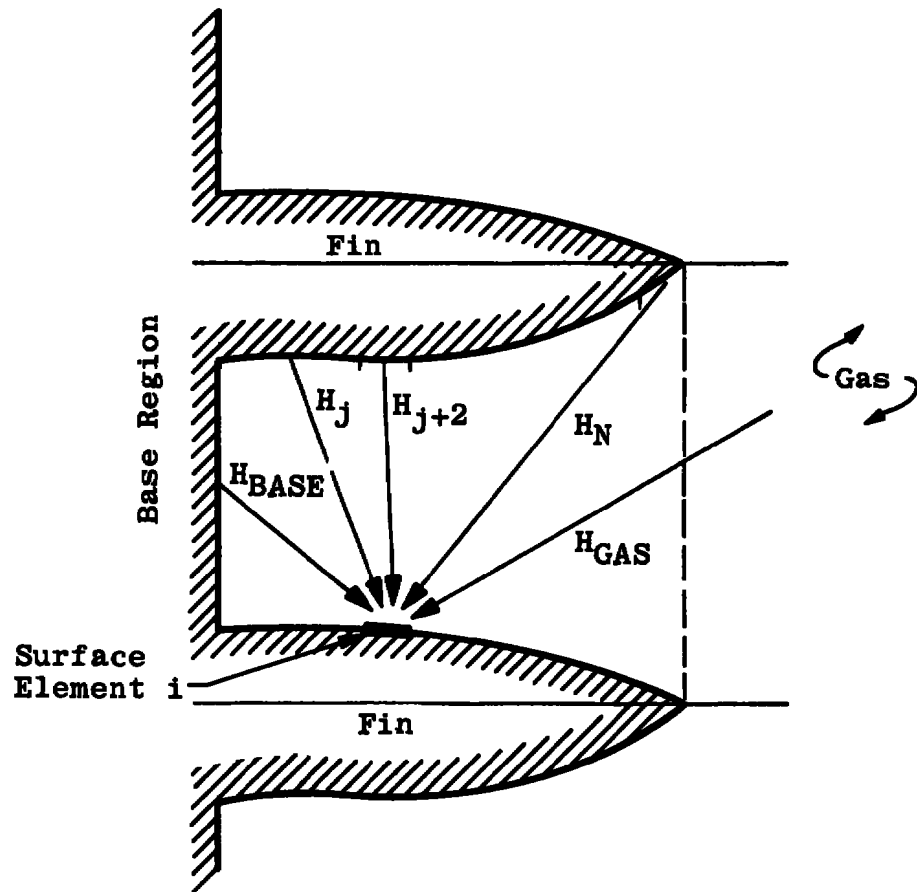


Figure 3. Cavity radiation.

outside the cavity. The term  $H_i$  in Equation 4 is seen to be the sum of all radiant energy arriving at the  $i$ 'th surface element. Denoting any other surface element as  $(j)$  and noting that the radiant energy which leaves  $(j)$  is in fact the radiosity of surface  $(j)$  leads to the conclusion that the radiosity of any surface element is dependent upon the radiosity of all other surface elements.

The radiation energy which leaves surface element  $(j)$  and which impinges on element  $(i)$  is given by Equation 5.

$$(Q_R)_{j \rightarrow i} = B_j F_{ji} \quad (5)$$

$F_{ji}$  is the shape factor which relates the per cent of energy leaving surface  $(j)$  that strikes surface  $(i)$ . Summing the radiative contribution of all surface elements to the irradiation of surface  $(i)$  leads to Equation 6.

$$H_i = \frac{1}{A_i} \sum_{j=1}^k B_j F_{ji} A_j = \sum_{j=1}^k B_j F_{ij} \quad (6)$$

Substitution of Equation 6 into Equation 4 and solving for the temperature term produces Equation 7.

$$\sigma T_i^4 = \frac{B_i}{\epsilon_i} - \frac{(1 - \epsilon_i)}{\epsilon_i} \sum_{j=1}^k B_j F_{ij} = \sum_{j=1}^k \left[ \frac{\delta_{ij} - (1 - \epsilon_i) F_{ij}}{\epsilon_i} B_j \right] \quad (7)$$

The term  $\delta_{ij}$  is the Kronecker delta which takes on the value

of one when  $j = i$  and which becomes zero when  $j \neq i$ .

Equation 7 now describes a system of  $(k)$  linear algebraic equations relating the element temperatures and element radiosities. Expressed in matrix notation, the system of equations is represented by Equation 8.

$$[\sigma T_i^4] = [\Omega_{ij}] [B_j] \quad (8)$$

The coefficient matrix elements  $\Omega_{ij}$  are given by

$\Omega_{ij} = [\delta_{ij} - (1 - \epsilon_i)F_{ij}] / \epsilon_i$ . Inversion of the coefficient matrix gives  $[\Omega_{ij}]^{-1} = [\chi_{ij}]$ . By employing the inverse matrix a new set of linear algebraic equations can be formed as represented by Equation 9.

$$[B_i] = [\chi_{ij}] [\sigma T_j^4] \quad (9)$$

Equation 9 now determines the radiosity of each surface element as a function of the temperatures of all the surface elements. It should be noted that the open end of the fin enclosure is considered a hypothetical surface of unit absorptivity which exists at the effective temperature of the gas.

The radiation energy flux leaving surface element  $(i)$  is given by Equation 10.

$$(q_R)_i = \epsilon_i \sigma T_i^4 - \alpha_i H_i \quad (10)$$

Substitution into Equation 10 for the value of the incident radiation as implied by Equation 4 gives Equation 11.

$$(q_R)_i = \epsilon_i \sigma T_i^4 - \alpha_i \left[ \frac{B_i - \epsilon_i \sigma T_i^4}{1 - \epsilon_i} \right] \quad (11)$$

Replacing the  $B_i$  term in Equation 11 with Equation 9 and recalling that for grey surfaces  $\alpha = \epsilon$  gives Equation 12, the final form of the heat flux relationship.

$$(q_R)_i = \sum_{j=1}^k \left[ \frac{\epsilon_i}{1 - \epsilon_i} \right] [\delta_{ij} - \chi_{ij}] \sigma T_j^4 = \sum_{j=1}^k \Lambda_{ij} \sigma T_j^4 \quad (12)$$

The term  $\Lambda_{ij}$  in Equation 12 is seen to be a function only of the particular geometry of the enclosure and the surface properties of the walls. The significant aspect of Equation 12 is that the heat flux from a surface element can be expressed in terms of the discrete distribution of temperature among the elements which make up the fin and base surfaces.

#### IV. NON-DIMENSIONALIZATION OF THE BASIC DIFFERENTIAL EQUATION

It now becomes convenient to non-dimensionalize the basic differential equation (Equation 2) and its associated boundary conditions (Equation 3). Letting the parameters  $K_c$ , and  $h_c$  represent characteristic values of thermal

conductivity and heat transfer coefficient respectively, and taking  $L$  as the fin length, the system is non-dimensionalized with the following dimensionless variables:

$$\begin{aligned}
 x &= \frac{x}{L} & y_1(x) &= \frac{y_1(x)}{L} & y_2(x) &= \frac{y_2(x)}{L} \\
 \bar{k}(x) &= \frac{k(x)}{k_c} & \bar{h}_1(x) &= \frac{h_1(x)}{h_c} & \bar{h}_2(x) &= \frac{h_2(x)}{h_c} \\
 \theta(x) &= \frac{T(x) - T_o}{T_{g\infty} - T_o} & \theta_{g1}(x) &= \frac{T_{g1}(x) - T_o}{T_{g\infty} - T_o} \\
 \theta_{g2}(x) &= \frac{T_{g2}(x) - T_o}{T_{g\infty} - T_o} & \bar{h}^*(1) &= \frac{h^*(L)}{h_c} \\
 Q_{R1}(x) &= \frac{q_{R1}(x) L}{k_c (T_o - T_{g\infty})} & Q_{R2}(x) &= \frac{q_{R2}(x) L}{k_c (T_o - T_{g\infty})} \\
 s &= \frac{s}{L}
 \end{aligned} \tag{13}$$

Substitution of Equation 13 into Equations 2 and 3 gives the following form of the basic differential equation:

$$f_2(x) \frac{d^2\theta}{dx^2} + f_1(x) \frac{d\theta}{dx} - f_o(x)\theta(x) = -[g_c(x) + g_R(x)] \tag{14}$$

The associated boundary conditions upon non-dimensionalization become as shown in Equations 15.

Boundary conditions:

$$1. \quad \theta(0) = 0.$$

$$2. \quad \frac{d\theta(1)}{dx} + \beta^*\theta(1) = \beta^*\bar{\theta}_g(1) - \frac{Q_R^*(1)}{K(1)}. \quad (15)$$

The functions  $f_2(x)$ ,  $f_1(x)$ ,  $f_0(x)$ ,  $g_c(x)$ , and  $g_R(x)$  are defined by the following equations:

$$f_2(x) = \bar{k}(x) [y_1(x) - y_2(x)]$$

$$f_1(x) = \left\{ \frac{\bar{k}(x)}{K(x)} \left[ \frac{dy_1(x)}{dx} - \frac{dy_2(x)}{dx} \right] + [y_1(x) - y_2(x)] \frac{d\bar{k}(x)}{dx} \right\} \\ = \frac{df_2(x)}{dx}$$

$$f_0(x) = N_C \left[ \bar{h}_1(x) \sqrt{1 + \left( \frac{dy_1(x)}{dx} \right)^2} + \bar{h}_2(x) \sqrt{1 + \left( \frac{dy_2(x)}{dx} \right)^2} \right]$$

$$g_c(x) = N_C \left[ \bar{h}_1(x) \sqrt{1 + \left( \frac{dy_1(x)}{dx} \right)^2} \theta_{g1}(x) \right. \\ \left. + \bar{h}_2(x) \sqrt{1 + \left( \frac{dy_2(x)}{dx} \right)^2} \theta_{g2}(x) \right]$$

$$g_R(x) = Q_{R1}(x) \sqrt{1 + \left( \frac{dy_1(x)}{dx} \right)^2} + Q_{R2}(x) \sqrt{1 + \left( \frac{dy_2(x)}{dx} \right)^2} \quad (16)$$

The parameters  $N_C$  and  $\beta^*$  are defined as follows:

$$N_C = \frac{h_c L}{K_C} \qquad \beta^* = \frac{h_c \bar{h}^* L}{K_C \bar{K}(1)}$$

The details of transforming Equations 2 and 3 into dimensionless form are given in Appendix A.

Two dimensionless parameters, the radiation number ( $N_R$ ), and the temperature ratio  $T_{g\infty}/T_O$  are now introduced by consideration of Equation 12. Putting Equation 12 into dimensionless form gives:

$$(Q_R)_i = N_R \sum_{j=1}^k \Lambda_{ij} \left[ \left( \frac{T_{g\infty}}{T_O} - 1 \right) \theta(X) + 1 \right]^4 \quad (17)$$

The radiation number is defined by  $N_R = \sigma T_O^4 L / K_C (T_O - T_{g\infty})$ .

#### V. TRANSFORMATION OF THE NON-DIMENSIONAL SYSTEM

Inspection of the second dimensionless boundary condition (Equation 15) indicates that this boundary condition has a non-zero right-hand side and hence is inhomogeneous. Application of the B. G. Galerkin technique requires that this boundary condition be homogeneous. Hence, it becomes necessary to transform the dimensionless system. Let the transformation variable  $[\psi(X)]$  be defined by Equation 18.

$$\psi(X) = \theta(X) - \left[ \beta^* \bar{\theta}_g(1) - \frac{Q_R^*}{\bar{K}(1)} \right] (X^2 - X) \quad (18)$$

Substitution of Equation 18 into Equations 14 and 15

yields the following transformed system:

$$\begin{aligned}
 & f_2(x) \frac{d\psi^2(x)}{dx} + f_1(x) \frac{d\psi(x)}{dx} - f_0(x) \psi(x) \\
 & = \left[ \beta^* \bar{\theta}_g(1) - \frac{Q_R^*}{\bar{K}(1)} \right] \left\{ (x^2 - x) f_0(x) - (2x - 1) f_1(x) - 2f_2(x) \right\} \\
 & - [g_c(x) + g_R(x)] \qquad \qquad \qquad (19)
 \end{aligned}$$

The associated transformed boundary conditions are given by Equation 20.

1.  $\psi(0) = 0.$
2.  $\frac{d\psi(1)}{dx} + \beta^* \psi(1) = 0.$  (20)

Equations 19 and 20 now define the mathematical system which will be solved through an iterative application of the B. G. Galerkin method.

## CHAPTER III

SOLUTION OF THE DEFINING EQUATION BY  
THE B. G. GALERKIN METHOD

## I. INTRODUCTION OF THE GALERKIN METHOD

The solution of the mathematical system is initiated by assuming that Equation 19 has a solution of the form indicated by Equation 21.

$$\psi(X) = a_1 \phi_1(X) + \sum_{i=2}^n a_i \phi_i(X) \quad (21)$$

where  $\phi_1$ , and  $\phi_i$  are assumed functions of X.

Equation 21 must satisfy the boundary conditions of the problem (Equation 19). Hence, Equations 22 must be satisfied.

$$\psi(0) = a_1 \phi(0) + \sum_{i=2}^n a_i \phi_i(0) = 0$$

$$\begin{aligned} \frac{d[\psi(1)]}{dX} + \beta * \psi(1) &= \frac{d}{dX} [a_1 \phi(1) + \sum_{i=2}^n a_i \phi_i(1)] \\ &+ \beta * [a_1 \phi_1(X) + \sum_{i=2}^n a_i \phi_i(1)] \\ &= 0 \end{aligned} \quad (22)$$

A form for the functions  $\phi_1(X)$  and  $\phi_i(X)$  is chosen as indicated by Equation 23:

$$\begin{aligned}\phi_1(X) &= (X - \gamma^*) X^2 \\ \phi_i(X) &= (1 - X)^2 X^{i-1}\end{aligned}\quad (23)$$

where  $\gamma^* = (3 + \beta^*) / (2 + \beta^*)$ .

Appendix B demonstrates that the assumed functions  $\phi_1$  and  $\phi_i$  do indeed satisfy the boundary conditions of the problem. The problem remains of evaluating the unknown coefficients  $a_1$  and  $a_i$  ( $i = 2, n$ ) appearing in the solution.

Substitution of the assumed solution into Equation 19 yields Equation 24.

$$\begin{aligned}& a_1 \left\{ f_2(X) (6X - 2\gamma^*) + f_1(X) (3X^2 - 2\gamma^*X) \right. \\ & \left. - f_0(X) (X^3 - \gamma^*X^2) \right\} + \sum_{i=2}^n a_i \left\{ [i(i+1)X^{i-1} \right. \\ & \left. - 2i(i-1)X^{i-2} + (i-1)(i-2)X^{i-3}] f_2(X) \right. \\ & \left. + [(i+1)X^i - 2iX^{i-1} + (i-1)X^{i-2}] f_1(X) \right. \\ & \left. - [X^{i+1} - 2X^i + X^{i-1}] f_0(X) \right\} \\ & = \left\{ \beta^* \bar{\theta}_g(1) - \frac{Q_R^*}{K(1)} \right\} [(X^2 - X) f_0(X) - (2X - 1) f_1(X) \\ & \left. - 2f_2(X)] - [q_C(X) + q_R(X)]\end{aligned}\quad (24)$$

Equation 24 is now a functional relationship in terms of the unknown constants  $a_1$  and  $a_i$ . Following the method detailed in Kantorovich and Krylov (18), the  $a$ 's can be solved for as the dependent variables of a linearly independent system of algebraic equations. The linear system is formed by multiplying Equation 24 through, in turn, by each function in the set  $\phi_i$  ( $i = 1, n$ ) and integrating the resulting equations between the limits of zero to one.

## II. FORMULATION OF THE ALGEBRAIC SYSTEM OF LINEAR EQUATIONS

Multiplying Equation 24 through by  $\phi_1(x)$  and integrating between the limits of zero to one gives Equation 25.

$$\begin{aligned}
 & a_1 [I_2(1,1) + I_1(1,1) - I_0(1,1)] \\
 & + \sum_{i=2}^n a_i [I_2(1,i) + I_1(1,i) - I_0(1,i)] \\
 & = \left\{ \beta \bar{\theta}_g(1) - \frac{Q_R^*}{K(1)} \right\} [J_0(1) - J_2(1) - J_1(1)] - G(1) \quad (25)
 \end{aligned}$$

The terms of the integrals  $I$ ,  $J$ , and  $G$  are defined as follows:

$$\begin{aligned}
 I_0(1,1) &= \int_0^1 f_0(x) (x^3 - \gamma x^2)^2 dx \\
 I_1(1,1) &= \int_0^1 f_1(x) (3x^2 - 2\gamma x) (x^3 - \gamma x^2) dx
 \end{aligned}$$

$$\begin{aligned}
I_2(1,1) &= \int_0^1 f_2(x) (6x - 2\gamma^*) (x^3 - \gamma^*x^2) dx \\
I_0(1,i) &= \int_0^1 f_0(x) (x^{i+1} - 2x^i + x^{i-1}) (x^3 - \gamma^*x^2) dx \\
I_1(1,i) &= \int_0^1 f_1(x) [(i+1)x^i - 2ix^{i-1} + (i-1)x^{i-2}] \\
&\quad \cdot (x^3 - \gamma^*x^2) dx \\
I_2(1,i) &= \int_0^1 f_2(x) [i(i+1)x^{i-1} - 2i(i-1)x^{i-2} \\
&\quad + (i-1)(i-2)x^{i-3}] (x^3 - \gamma^*x^2) dx \\
J_0(1) &= \int_0^1 (x^2 - x) f_0(x) (x^3 - \gamma^*x^2) dx \\
J_1(1) &= \int_0^1 (2x - 1) f_1(x) (x^3 - \gamma^*x^2) dx \\
J_2(1) &= \int_0^1 2f_2(x) (x^3 - \gamma^*x^2) dx \\
G(1) &= \int_0^1 g_R(x) (x^3 - \gamma^*x^2) dx + \int_0^1 g_C(x) (x^3 - \gamma^*x^2) dx
\end{aligned} \tag{26}$$

Expressing Equation 25 in a shorthand notation leads to Equation 27:

$$a_1[z(1,1)] + \sum_{i=2}^n a_i[z(1,i)] = zH(1) \tag{27}$$

The elements of Equation 27 are defined as follows:

$$Z(1,1) = [I_2(1,1) + I_1(1,1) - I_0(1,1)]$$

$$Z(1,i) = [I_2(1,i) + I_1(1,i) - I_0(1,i)]$$

$$ZH(1) = \left\{ \beta^* \bar{\theta}_g(1) - \frac{Q_R^*}{K(I)} \right\} [J_0(1) - J_2(1) - J_1(1)] - G(1) \quad (28)$$

In a similar manner multiplying Equation 24 through, in turn, by each of the functions  $\phi_i$  ( $i = 2, n$ ) and integrating between the limits of zero to one produces a system of algebraic equations represented by Equation 29.

$$\begin{aligned} & a_1 [I_2(k,1) + I_1(k,1) - I_0(k,1)] \\ & + \sum_{i=2}^n a_i [I_2(k,i) + I_1(k,i) - I_0(k,i)] \\ & = \left\{ \beta^* \bar{\theta}_g(1) - \frac{Q_R^*}{K(I)} \right\} [J_0(k) - J_2(k) - J_1(k)] - G(k) \end{aligned} \quad (29)$$

The elements of Equation 29 are defined as follows:

$$I_0(k,1) = \int_0^1 f_0(x) (x^3 - \gamma^* x^2) (x^{k+1} - 2x^k + x^{k-1}) dx$$

$$I_1(k,1) = \int_0^1 f_1(x) (3x^2 - 2\gamma^* x) (x^{k+1} - 2x^k + x^{k-1}) dx$$

$$I_2(k,1) = \int_0^1 f_2(x) (6x - 2\gamma^*) (x^{k+1} - 2x^k + x^{k-1}) dx$$

$$\begin{aligned}
I_0(k, i) &= \int_0^1 f_0(x) [x^{i+1} - 2x^i + x^{i-1}] \\
&\quad \cdot (x^{k+1} - 2x^k + x^{k-1}) dx \\
I_1(k, i) &= \int_0^1 f_1(x) [(i+1)x^i - 2ix^{i-1} + (i-1)x^{i-2}] \\
&\quad \cdot (x^{k+1} - 2x^k + x^{k-1}) dx \\
I_2(k, i) &= \int_0^1 f_2(x) [i(i+1)x^{i-1} - 2i(i-1)x^{i-2} \\
&\quad + (i-1)(i-2)x^{i-3}] (x^{k+1} - 2x^k + x^{k-1}) dx \\
J_0(k) &= \int_0^1 (x^2 - x) f_0(x) (x^{k+1} - 2x^k + x^{k-1}) dx \\
J_1(k) &= \int_0^1 f_1(x) (2x - 1) (x^{k+1} - 2x^k + x^{k-1}) dx \\
J_2(k) &= \int_0^1 2f_2(x) (x^{k+1} - 2x^k + x^{k-1}) dx \\
G(k) &= \int_0^1 g_R(x) (x^{k+1} - 2x^k + x^{k-1}) dx \\
&\quad + \int_0^1 g_C(x) (x^{k+1} - 2x^k + x^{k-1}) dx \tag{30}
\end{aligned}$$

Expressing Equation 29 in a shorthand notation leads

to Equation 31:

$$a_1 [Z(k,1)] + \sum_{i=2}^n a_i [Z(k,i)] = [ZH(k)] \quad (31)$$

The elements of Equation 31 are defined as follows:

$$Z(k,1) = [I_2(k,1) + I_1(k,1) - I_0(k,1)]$$

$$Z(k,i) = [I_2(k,i) + I_1(k,i) - I_0(k,i)]$$

$$ZH(k) = \left\{ \beta^* \bar{\theta}_g(1) - \frac{Q_R^*}{K(1)} \right\} [J_0(k) - J_2(k) - J_1(k)] - G(k) \quad (32)$$

Equations 27 and 31 now represent a system of  $n$  linear algebraic equations containing the  $n$  unknown  $a_i$ 's. Expressed in matrix notation the system is represented by Equation 33.

$$\sum_{m=1}^n Z_{\ell,m} a_m = ZH_{\ell} \quad \text{with } \ell = 1, n \quad (33)$$

which upon solving for the  $a$ 's becomes

$$a_{\ell} = \sum_{m=1}^n Z_{\ell,m}^{-1} ZH_m \quad (34)$$

### III. SOLUTION OF THE ALGEBRAIC SYSTEM OF LINEAR EQUATIONS

The  $Z_{\ell,m}$  matrix elements of Equation 33 are functions of fin geometry and the assumed form of the  $\phi_i(X)$  functions. Hence, once the fin geometry is fixed, the  $Z_{\ell,m}$  elements can be evaluated and the inverse computed.

Equations 16, 26, 28, and 32 indicate that the  $[ZH]_m$  elements depend upon the radiative heat transfer from the fin which is in turn dictated by the temperature distribution along the fin. Hence, the solution of the linear system of equations for the a's requires an iterative process.

A simplified outline of the computation steps necessary to achieve a solution based upon a selected set of fin parameters are enumerated as follows:

1. Evaluate the  $Z_{\ell,m}$  matrix elements and compute the inverse matrix  $Z_{\ell,m}^{-1}$  for the selected fin geometry.
2. Assume the radiative heat transfer from the fin is zero and calculate an initial temperature distribution in the fin based on convective interactions only.
3. Using the temperature distribution computed in step 2, evaluate the radiative heat transfer from Equations 8 through 12 and Equation 17.
4. Using the calculated radiation heat transfer, evaluate the ZH elements and calculate a new temperature distribution in the fin.

5. Recalculate radiative heat transfer using the temperature distribution from step 4.

6. Repeat steps 4 and 5 until the solution converges.

The method of solution presented in Chapters II and III has been programmed in G level Fortran on the IBM 360/50 computer. Appendix C is a Fortran listing of the computer program.

## CHAPTER IV

APPLICATION OF THE SOLUTION TECHNIQUE  
TO FINS OF SELECTED SHAPEI. DESCRIPTION OF SELECTED FIN SHAPES  
AND CONDITIONS OF ANALYSIS

The foregoing method of solution was applied to fins of parabolic, triangular, and inverse parabolic profile. The dimensionless area of each profile was held constant at 0.2 which assures the same volume per unit depth of fin. Thus a comparison of the reported fin performance can be made on an equivalent weight per fin basis.

The selected fins were analyzed for the case of constant thermal conductivity, negligible convective heat transfer, and a ratio of gas temperature to base temperature,  $T_{g\infty}/T_o$ , equal to zero. These latter conditions correspond closely to those encountered in space. Other geometrical, environmental, and surface property parameters varied, as are enumerated below:

1. Non-dimensional fin spacing,  $S$ , was assigned values of 0.5, 1.0, 2.0, 4.0, and 6.0.
2. The radiation number,  $N_R$ , was assigned values of 0.1, 0.5, 1.0, and 5.0.
3. Fin surface emissivity and base emissivity were set equal and were assigned the values of 0.2, 0.5, and 0.8.

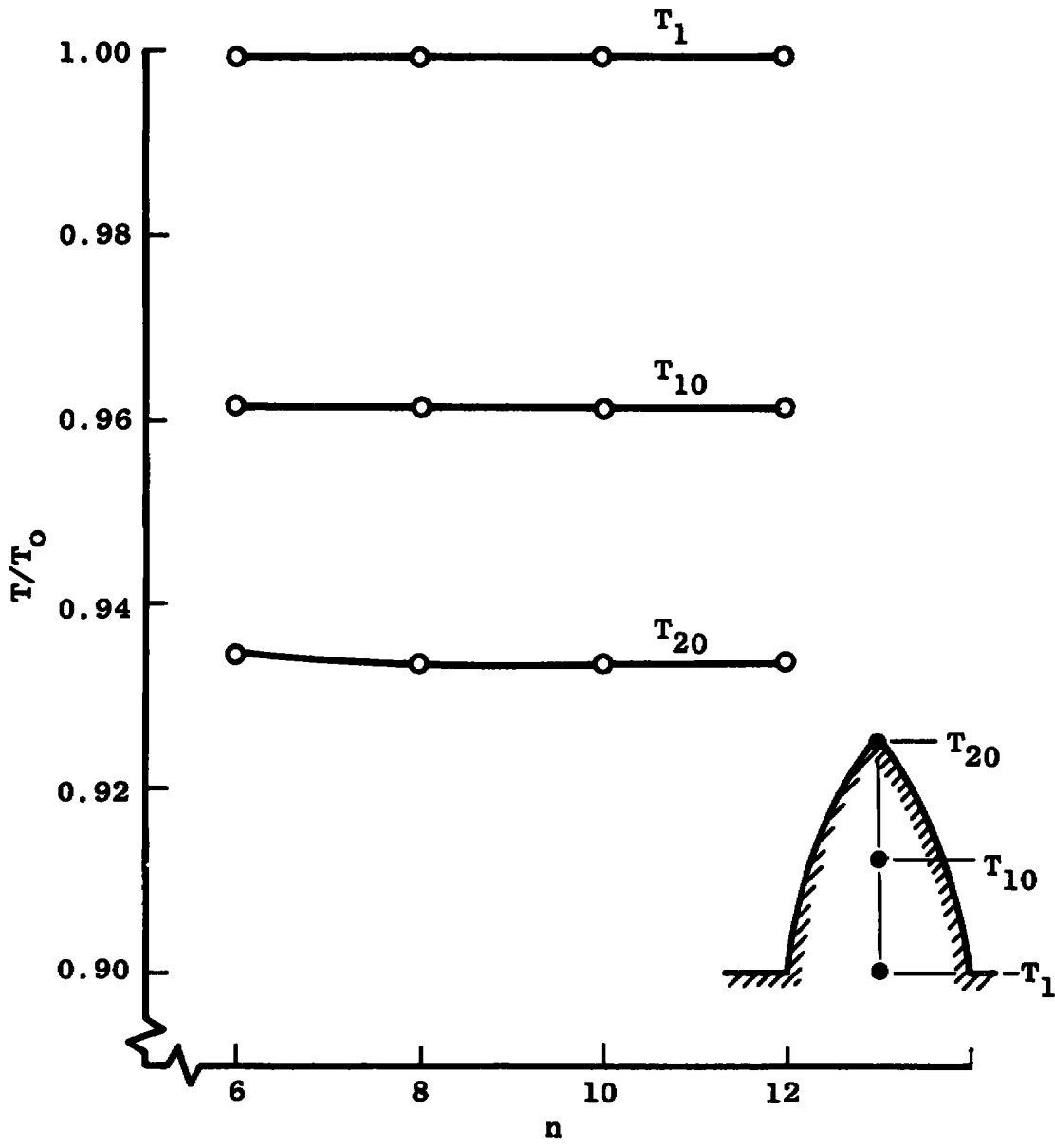
The total number of cases analyzed was 180.

## II. DESCRIPTION OF SELECTED MATHEMATICAL PARAMETERS

For the radiative heat transfer calculations the fin surfaces were divided into forty elements and the base area between fins into five elements. The number,  $n$ , of approximating functions,  $\phi$ , used in the Galerkin solution was ten. Values of  $n$  larger than ten were found to give no improvement to the first four significant digits in the solution for the temperature distribution. Figure 4 illustrates the effect of variations in  $n$  on the solution for temperature at specific locations along the fin.

To facilitate convergence of the iterative method,  $\theta$  was bounded between +2.0 and -1.0. The physical bounds on  $\theta$ , +1.0 and zero, were exceeded in the solution in order to stabilize the convergence; since as the solution progressed, values assigned to  $\theta$  were the accumulated average of all preceding iterations.

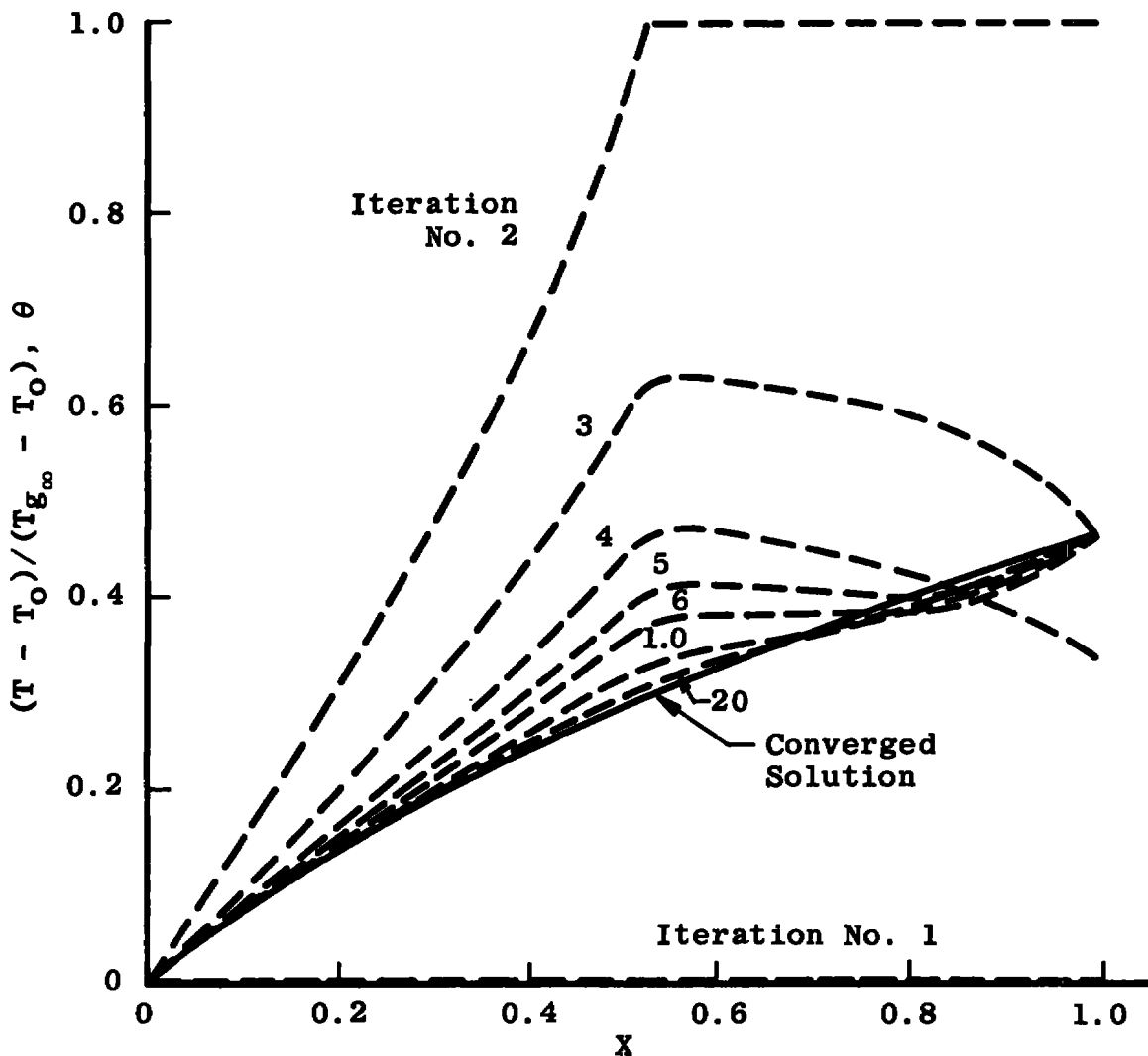
The convergence criterion employed required that the value of heat flux for each fin element should change by no more than 0.1 per cent during successive iterations. The computer was programmed to run for thirty iterations or until the solution converged. Each iteration required approximately three seconds, and the average number of iterations required per solution was twenty.



Fin Configuration            Parabolic  
 Fin Spacing, S              5.0  
 Surface Emissivity,  $\epsilon$     0.2  
 Radiation Number,  $N_R$     0.1  
 $\frac{T_{g\infty}}{T_0} = 0.0$

Figure 4. Effects of n on the solution for temperature distribution.

Cases involving high values of surface emissivity, high  $N_R$ , and fin spacing greater than 4.0 did not always converge in thirty iterations. These cases were rerun with fifty iterations and in all cases converged to an acceptable solution. Figure 5 shows the convergence of the temperature distribution for a typical fin configuration. Bounding of the temperature distribution at the upper bound is indicated for the second iteration in Figure 5.



Fin Configuration	Inverse Parabolic
Fin Spacing, S	1.0
Surface Emissivity, $\epsilon$	0.2
Radiation Number, $N_R$	5.0
$\frac{T_{g\infty}}{T_0} = 0.0$	

Figure 5. Convergence of successive iterations.

## CHAPTER V

## PRESENTATION AND DISCUSSION OF RESULTS

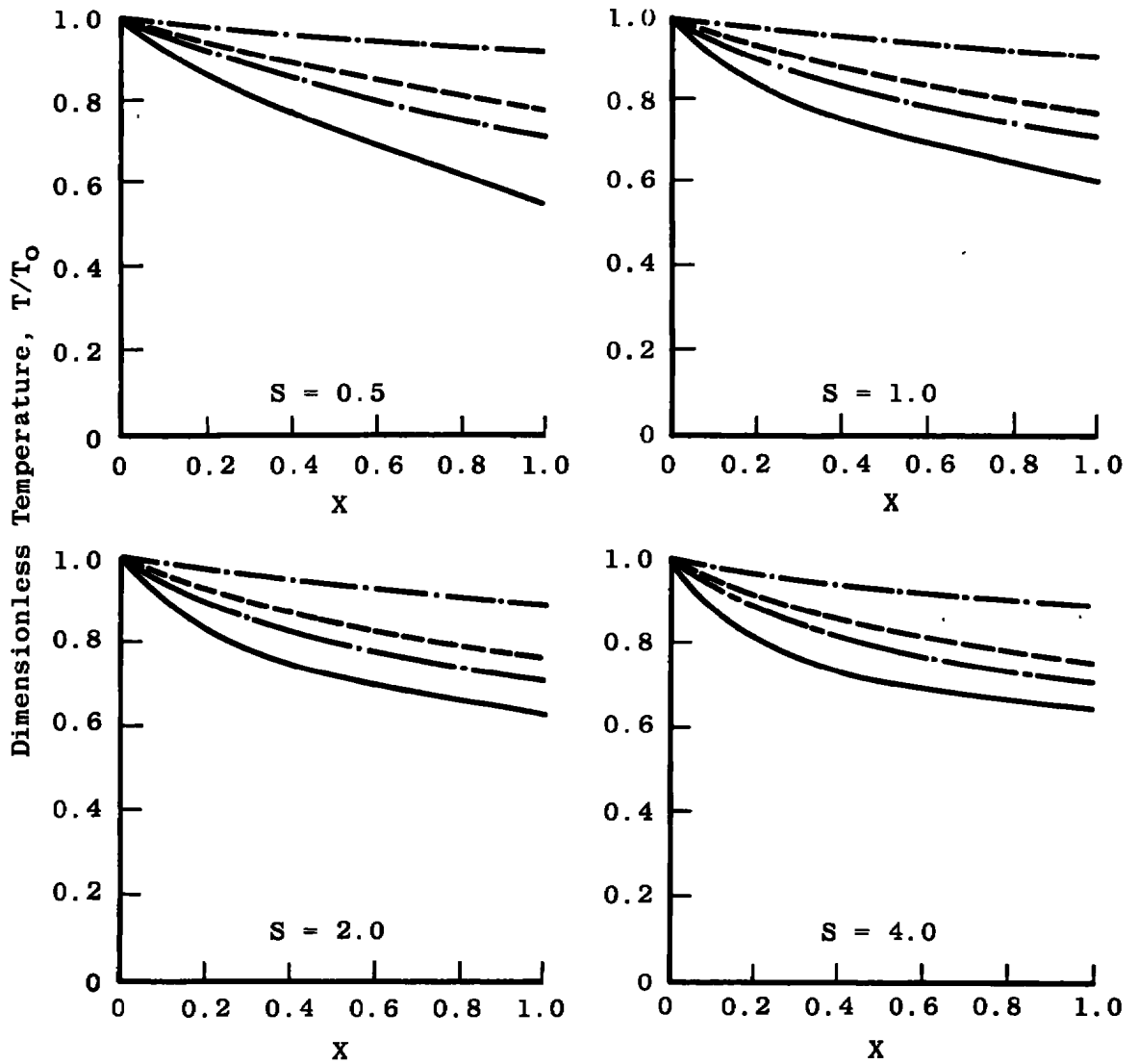
## I. TEMPERATURE DISTRIBUTION

The non-dimensional temperature distribution,  $T/T_0$ , for each combination of  $S$ ,  $N_R$ , and  $\epsilon$  are shown in Figures 6, 7, and 8 for the parabolic, triangular, and inverse parabolic fins, respectively.

The effect of fin spacing on temperature distribution is seen to depend upon surface emissivity. For low surface emissivity,  $\epsilon = 0.2$ , heating of the fin by radiation from the base is appreciably reduced because of the high reflectivity of the surface. As surface emissivity increases, fin spacing is seen to have a greater influence on temperature distribution. Physically, this effect is attributable to increased absorption of base radiation by the fin. As spacing increases, the fin can see larger areas of the base, and hence, absorbs more of the radiation from the base. The overall temperature drop along the fin becomes less as spacing increases; since as radiation energy input increases, the conduction of energy along the fin must decrease.

Because of the much larger shape factor between the base and the inverse parabolic fin, a greater influence of fin spacing is observed. It is interesting to note that for





Symbol	$N_R$	$N_C = 0.0$
· · · · ·	0.1	$\epsilon = 0.5$
- - - - -	0.5	$\frac{T_{g\infty}}{T_0} = 0.0$
- · - · -	1.0	
—————	5.0	

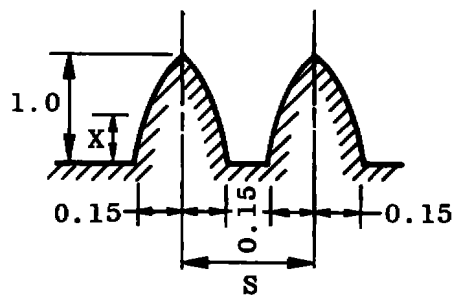


Figure 6 (continued)

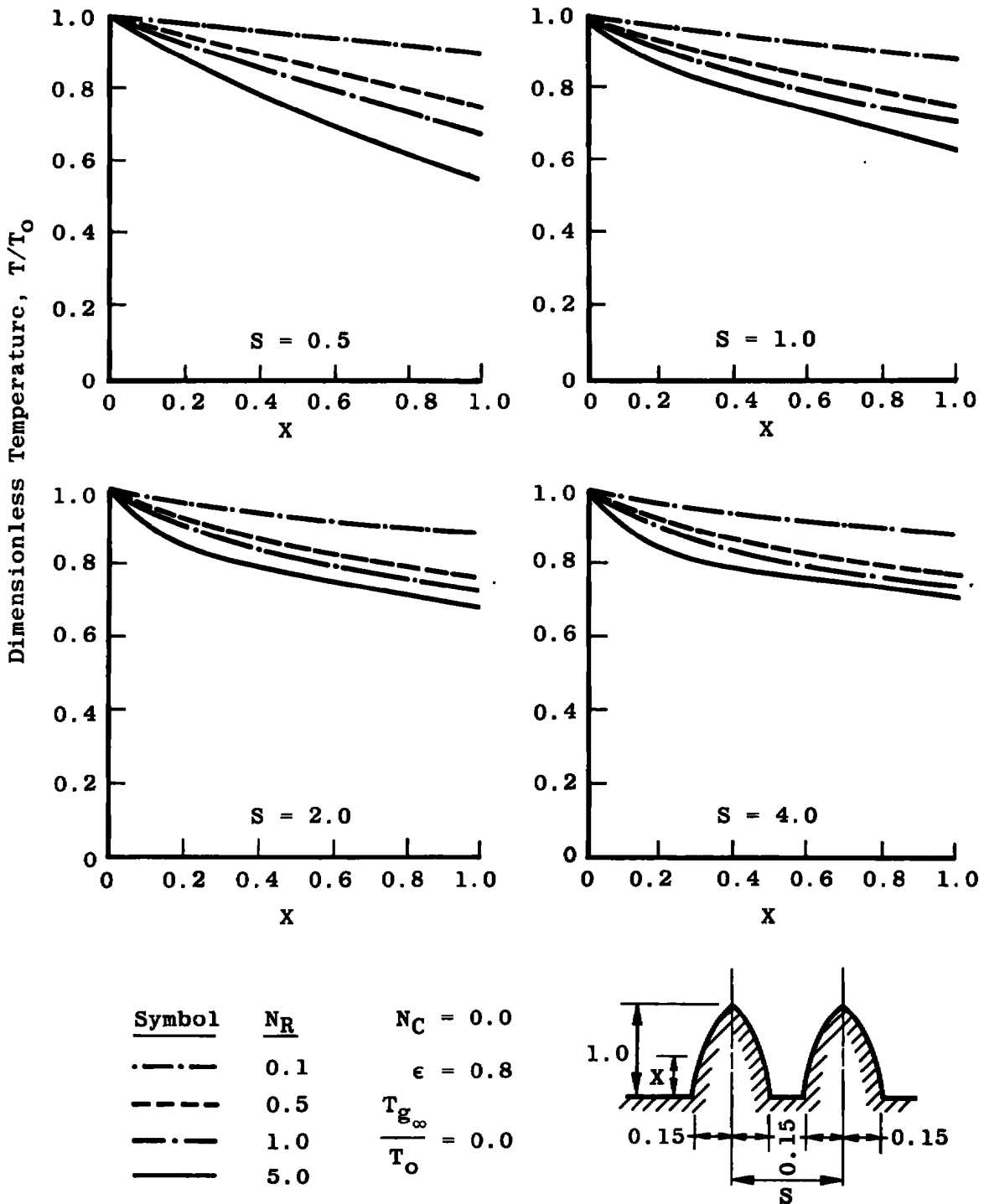


Figure 6 (continued)

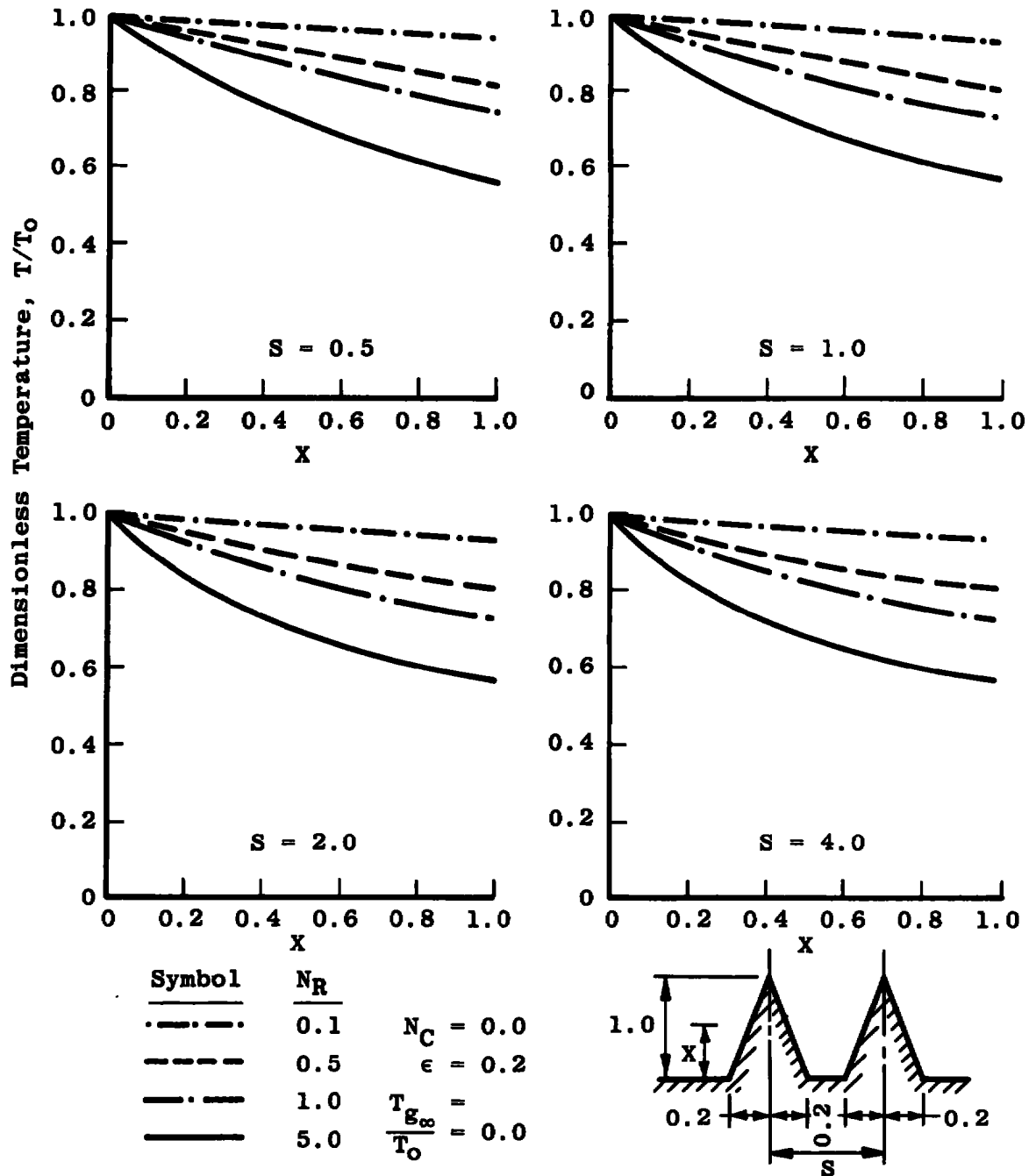


Figure 7. Dimensionless temperature distribution in a triangular fin.

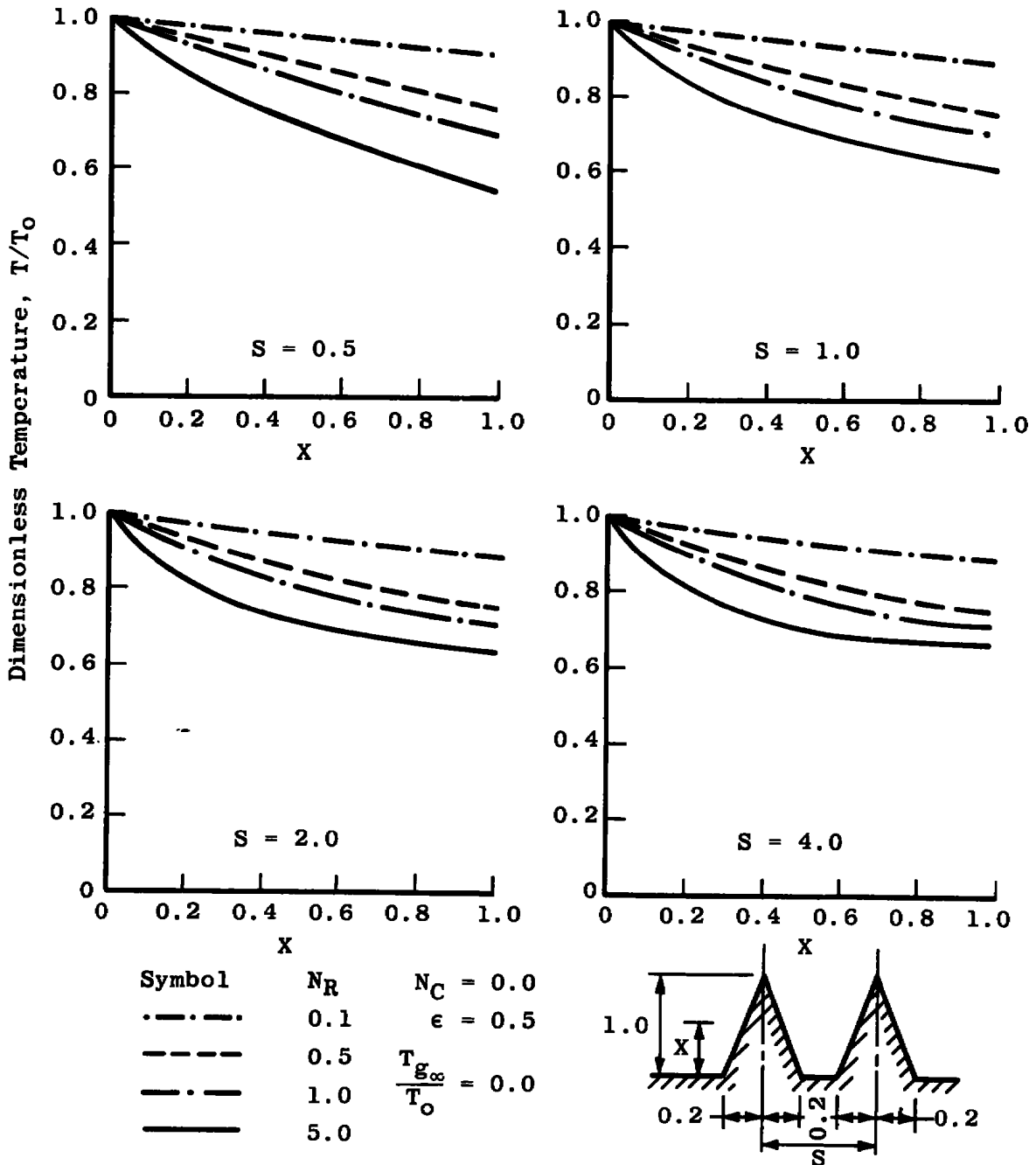


Figure 7 (continued)

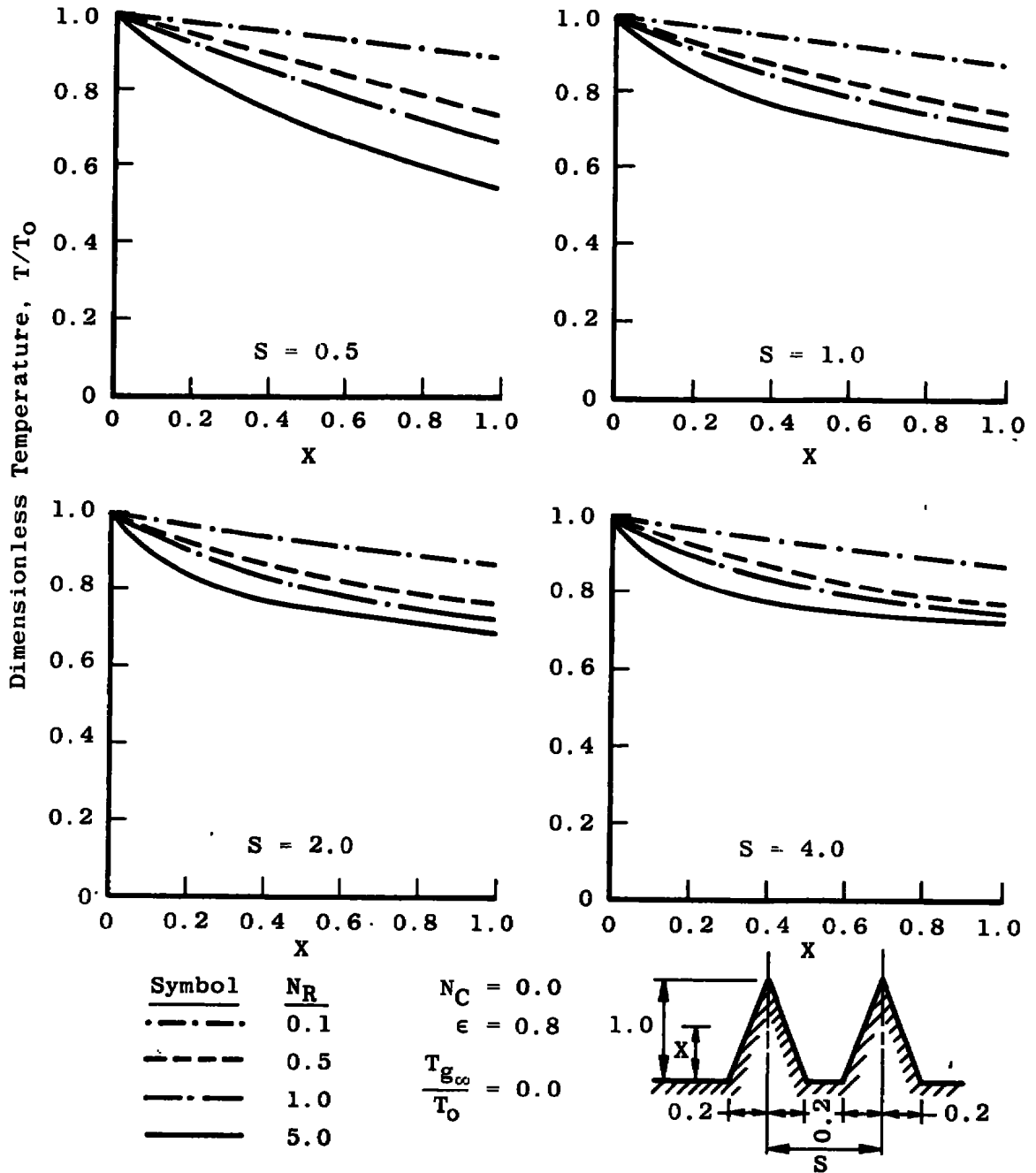


Figure 7 (continued)

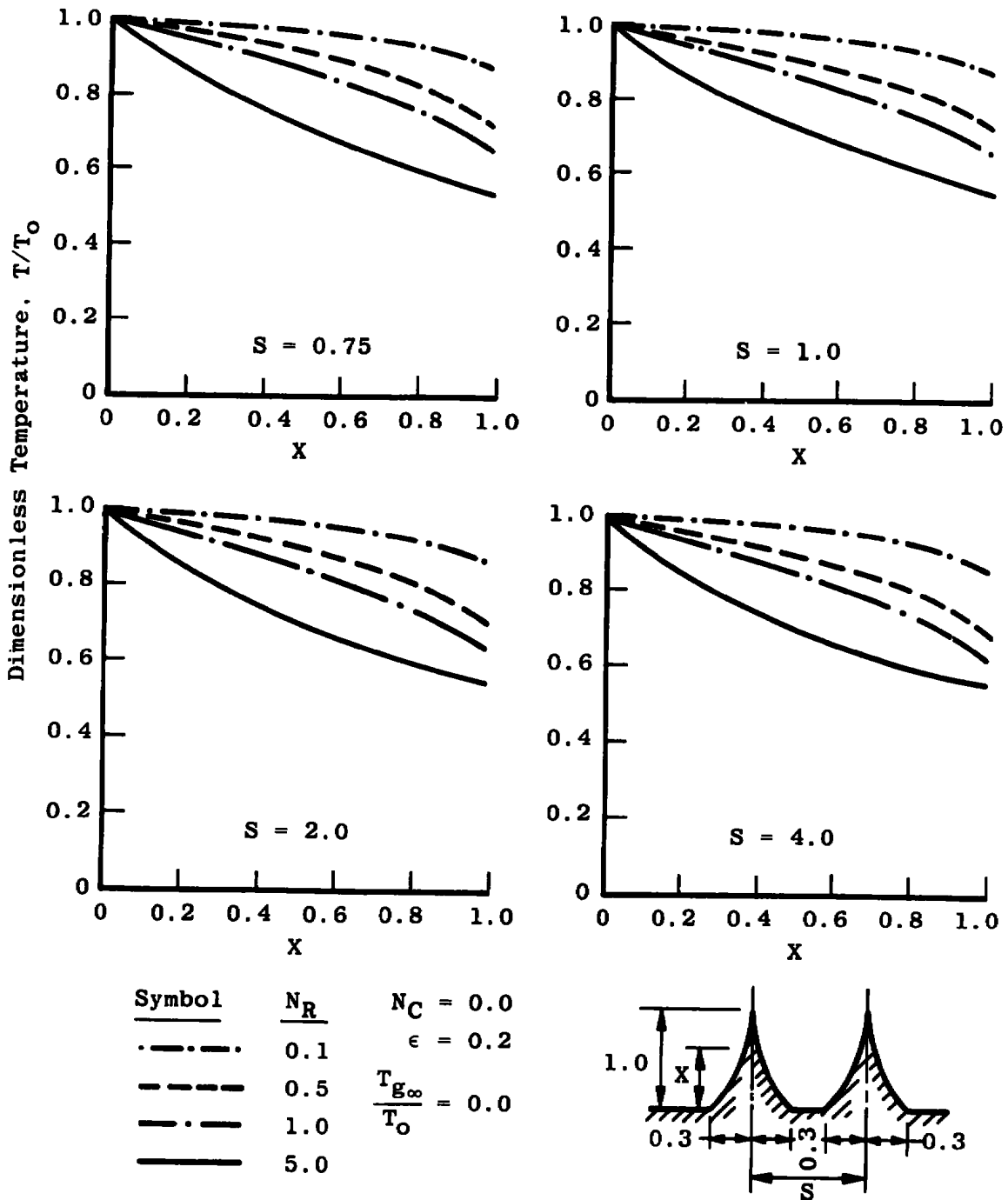


Figure 8. Dimensionless temperature distribution in an inverse parabolic fin.

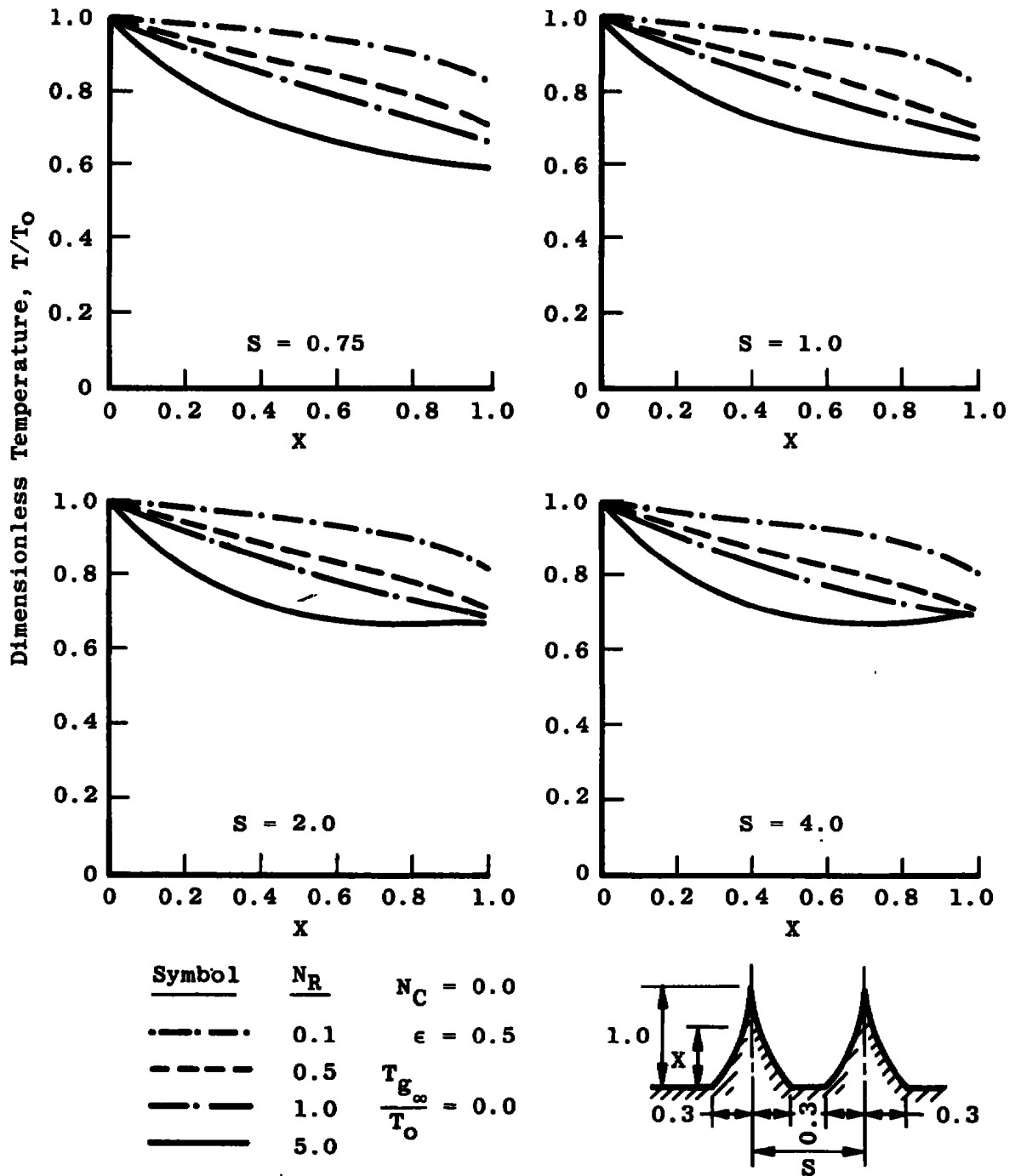


Figure 8 (continued)

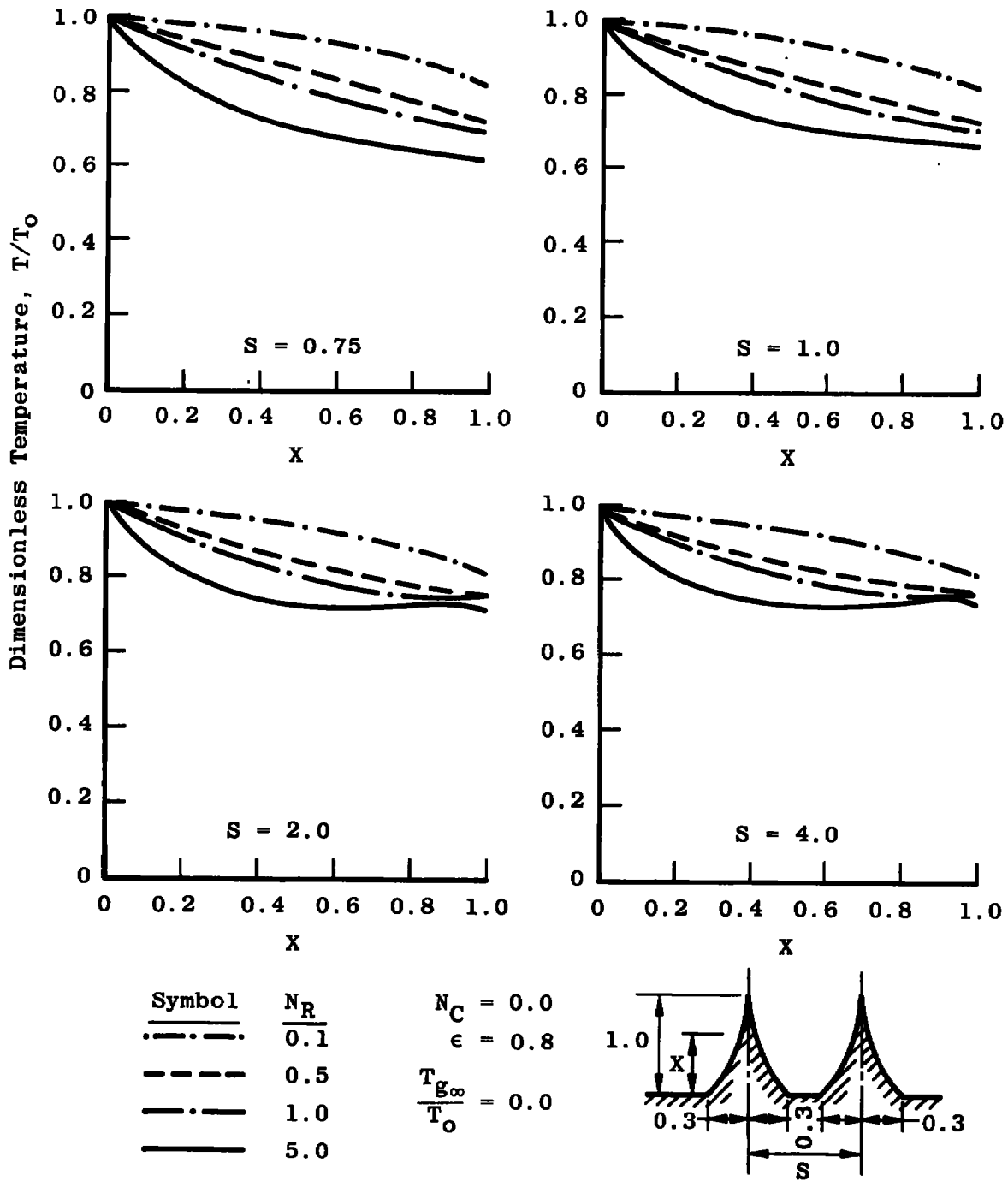


Figure 8 (continued)

high values of  $S$ ,  $N_R$ , and  $\epsilon$  the temperature gradient actually reverses near the two-thirds point on the fin. This indicates that the tip region is heated by radiation from the base at a rate faster than it is cooled by reemission to the gas, and thus heat is conducted in the negative direction along the fin to a region where the cooling rate is higher.

Two types of heat transfer phenomena, conduction and radiation, occur in the radiation fin. The radiation number,  $N_R$ , being a ratio of radiation to conduction effects, is a measure of the dominating mode of heat transfer. For  $N_R$  approaching zero, the heat transfer process becomes radiation limited since the fin can conduct more heat internally along the fin than can be radiated away. Conversely for  $N_R$  greater than one, the process becomes conduction limited. These limits are clearly demonstrated by Figures 6, 7, and 8 where temperature distributions for low  $N_R$  are not appreciably affected by either surface emissivity or fin spacing; while for large  $N_R$ , a strong influence on temperature distribution is exerted by both surface emissivity and fin spacing.

## II. FIN EFFICIENCY

So that the performance of arrays of different fin configurations might be studied and compared, it becomes necessary to define certain fin performance parameters.

One such parameter is the fin efficiency,  $\eta$ , defined as the ratio of the combined convective and radiative heat transfer from a single fin to the hypothetical combined convective and radiative heat transfer from a fin of similar geometry with black surfaces and with infinite thermal conductivity. Expressed in terms of the dimensionless variables, the fin efficiency becomes

$$\begin{aligned}
 \eta = & \int_0^1 \{Q_{R1}(x) + N_C[1 - \theta_1(x)]\} \sqrt{1 + \left(\frac{dy_1(x)}{dx}\right)^2} dx \\
 & + \int_0^1 \{Q_{R2}(x) + N_C[1 - \theta_2(x)]\} \sqrt{1 + \left(\frac{dy_2(x)}{dx}\right)^2} dx \\
 & + [Y_1(x) - Y_2(x)]\{Q_R^* + N_C[1 - \theta(1)]\} \\
 & \cdot \int_0^1 \left\{ N_R[1 - (T_o/T_{g\infty})^4 + N_C] \left[ \sqrt{1 + \left(\frac{dy_1(x)}{dx}\right)^2} \right. \right. \\
 & \left. \left. + \sqrt{1 + \left(\frac{dy_2(x)}{dx}\right)^2} \right] dx \right\}^{-1}
 \end{aligned} \tag{35}$$

Fin efficiencies are calculated for each fin configuration and presented in Figures 9, 10, and 11 for selected values of  $S$ ,  $N_R$ , and  $\epsilon$ . The fin efficiency is seen to vary

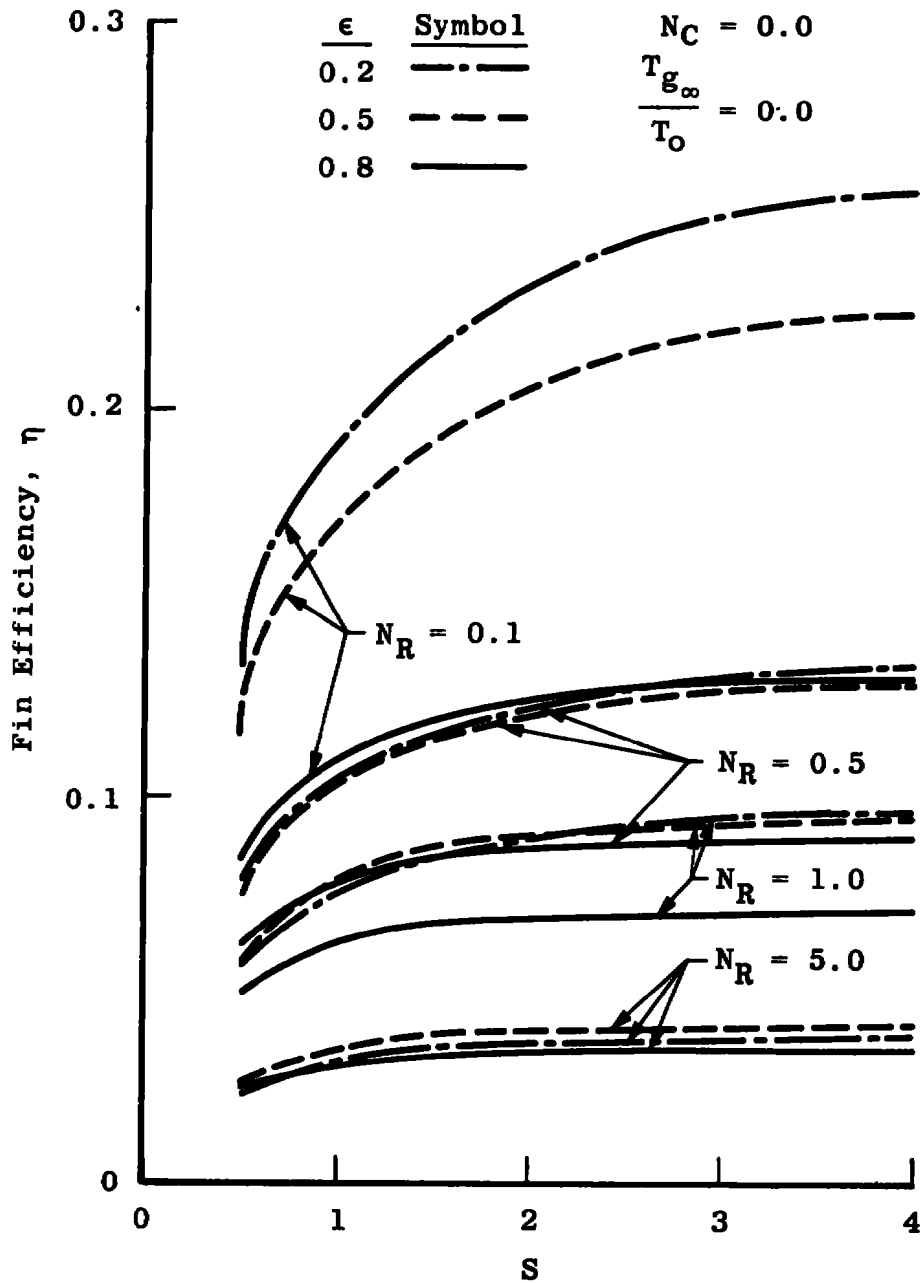


Figure 9. Parabolic fin efficiency.

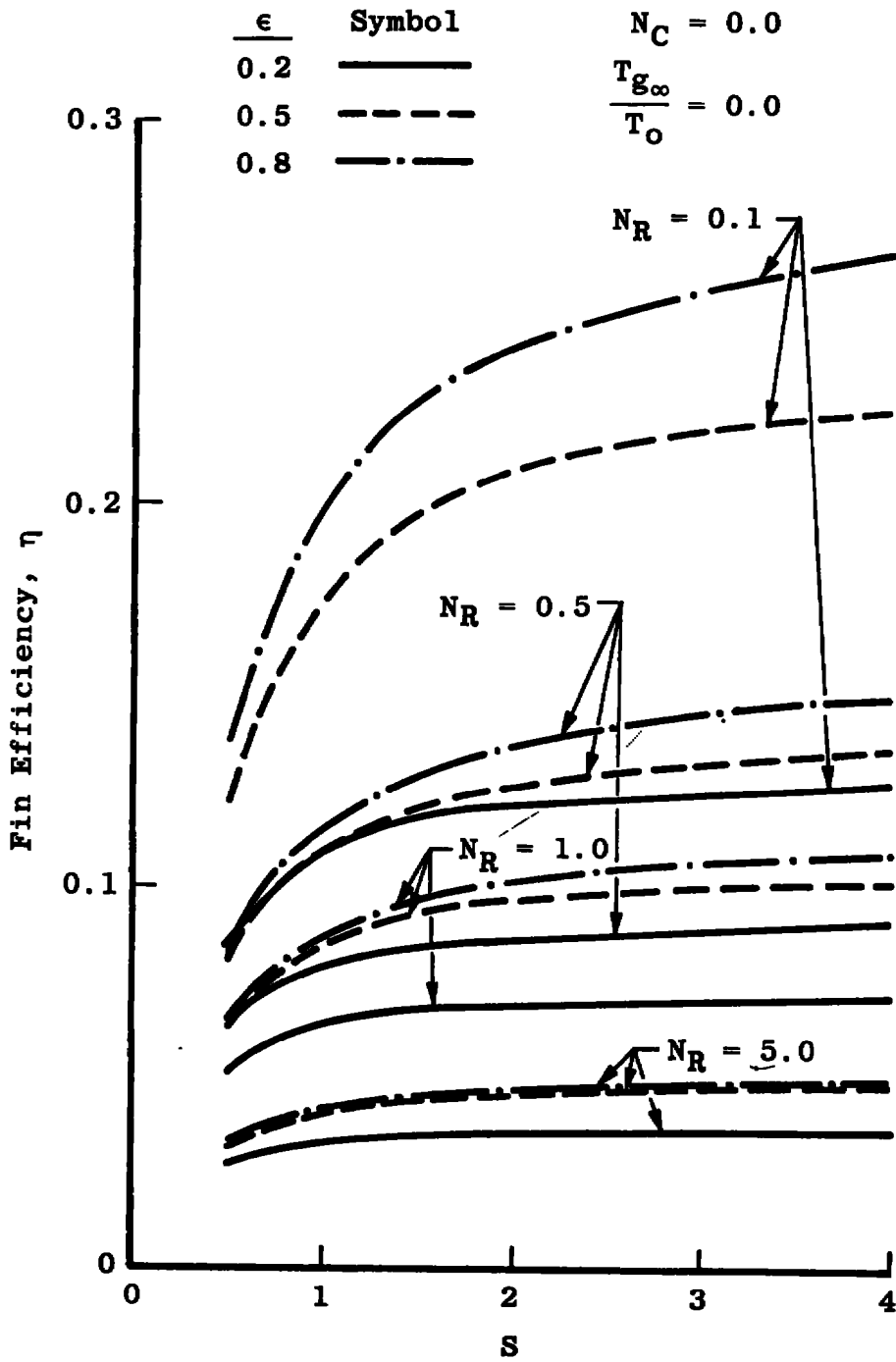


Figure 10. Triangular fin efficiency.

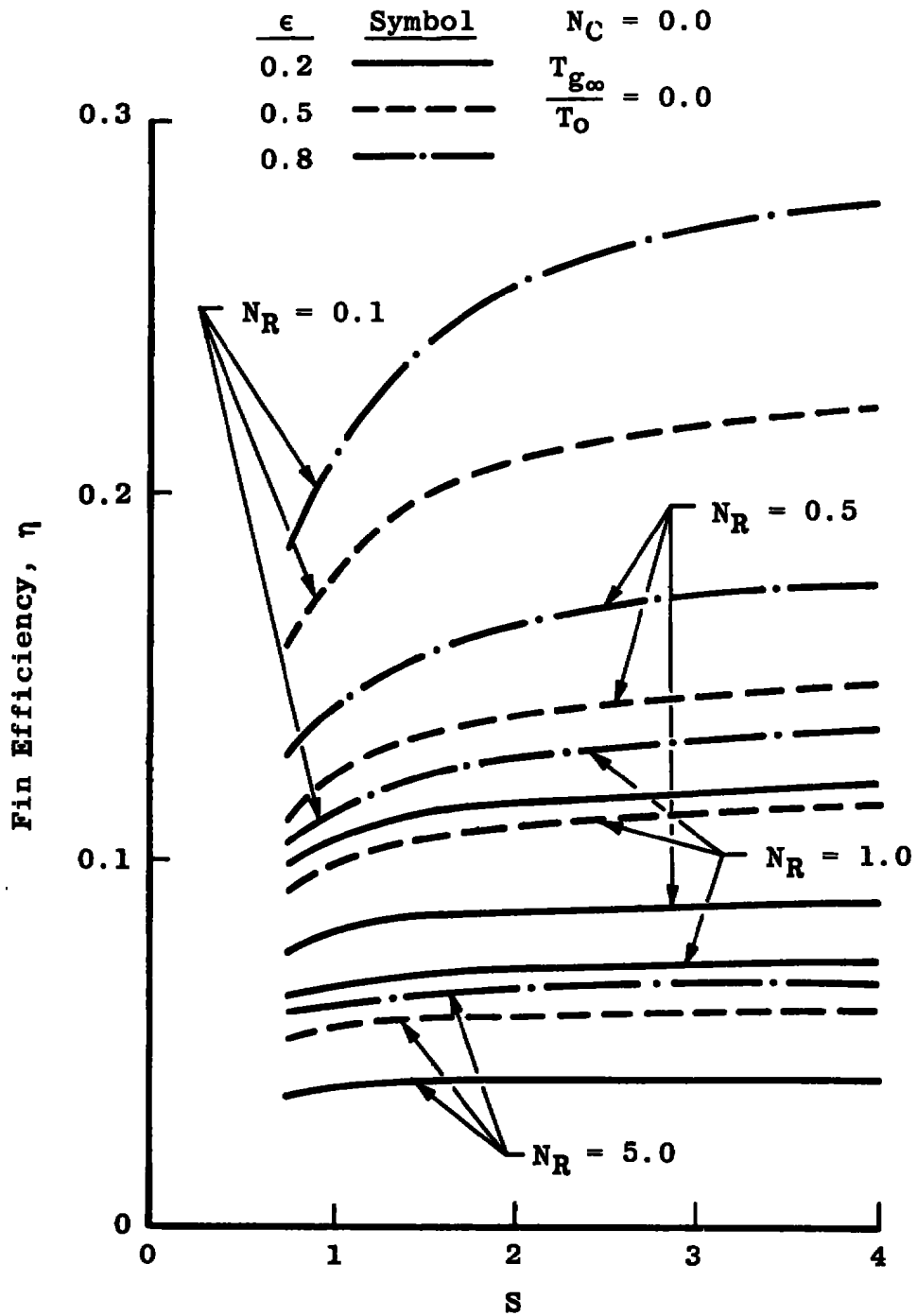


Figure 11. Inverse parabolic fin efficiency.

directly with surface emissivity, inversely with  $N_R$ , and to increase with  $S$ , asymptotically approaching some maximum and limiting value. The limiting value corresponds to the efficiency of a single fin situated on a base of infinite dimensions, and free of interactions with adjacent fins.

Limiting values of fin efficiency occur at a spacing of about 2.0 for a  $N_R$  of 5.0, and at a spacing of about 4.0 for a  $N_R$  of 0.1. An explanation for the maximum and limiting values of fin efficiency is found by considering that as spacing increases, the fins interact less with adjacent fins and more with the warmer base region. Increased interactions with the base cause the overall fin temperature to rise because of higher rates of radiation energy input from the base. Further spacing cannot influence the fin temperature once the point is reached where adjacent fins no longer interact, since the fin is now fully interacting with the base. At this point, the fin has a maximum temperature and is emitting energy at the highest possible rate and, hence, has the highest possible efficiency.

Fin efficiency can lead to serious misinterpretation of fin performance since it assumes that all energy leaving the fin also leaves the enclosure formed by the adjacent fins and the base. When interactions are present, this assumption is false and can lead to contradicting conclusions regarding optimum fin configurations.

A more valid parameter for measuring the performance

of arrays of longitudinal fins is the apparent emittance.

### III. APPARENT EMITTANCE

A measure of the performance of a fin cluster is the apparent emittance,  $\epsilon_A$ . Apparent emittance is defined as the ratio of the actual rate of radiation energy efflux from the mouth of the cavity between two adjacent fins, to the rate of radiation energy efflux from a black surface at the uniform temperature condition of the wall,  $T_o$ , and having an area equal to that of the mouth of the cavity. Expressed in terms of the dimensionless variables, the apparent emittance becomes:

$$\begin{aligned} \epsilon_A = & \int_0^1 \left\{ Q_{R1}(X) \sqrt{1 + \left( \frac{dy_1(X)}{dX} \right)^2} \right. \\ & \left. + Q_{R2}(X) \sqrt{1 + \left( \frac{dy_2(X)}{dX} \right)^2} \right\} dX + \int_{\text{Base}} Q_{R-\text{Base}} dA_{\text{Base}} \\ & \cdot \left[ N_R [1 - (T_{g\infty}/T_o)^4] \{ S - [Y_1(0) - Y_2(0)] \} \right]^{-1} \end{aligned} \quad (36)$$

Apparent emittances were calculated for each fin configuration and presented in Figures 12, 13, and 14 for selected values of  $S$ ,  $N_R$ , and  $\epsilon$ .

As would be expected, the apparent emittance,  $\epsilon_A$ , is

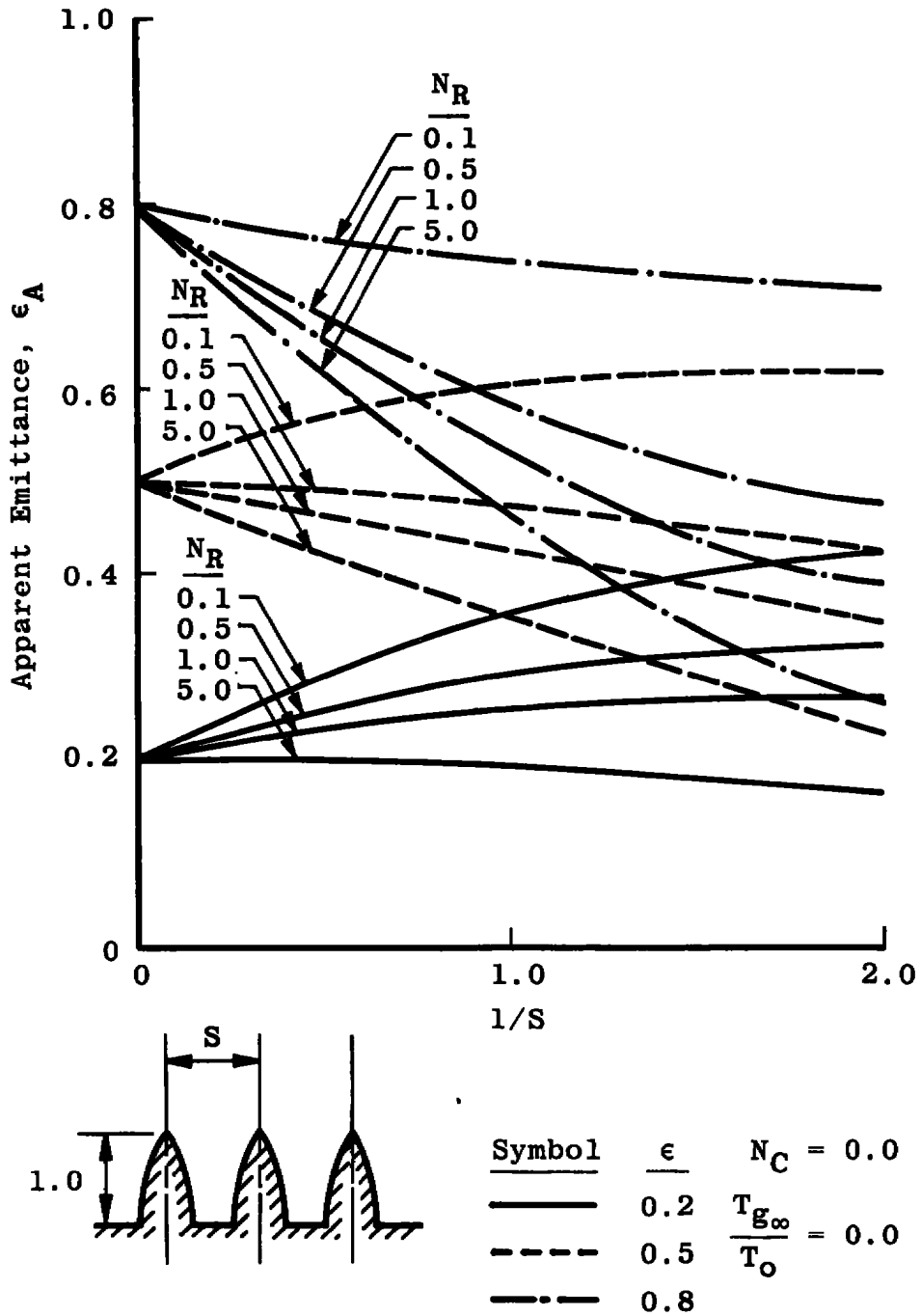


Figure 12. The apparent emittance of a parabolic fin cluster.

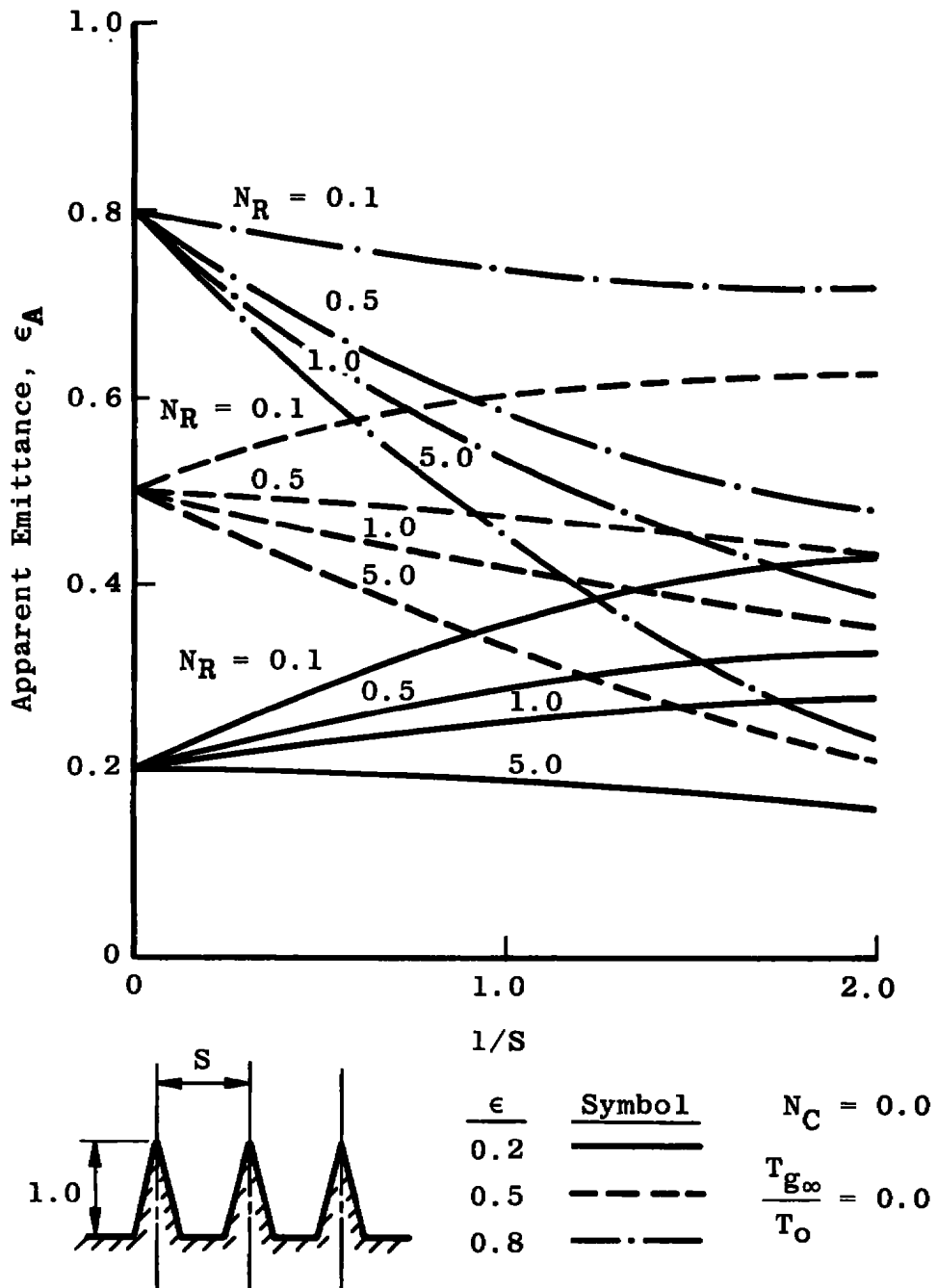


Figure 13. The apparent emittance of a triangular fin cluster.

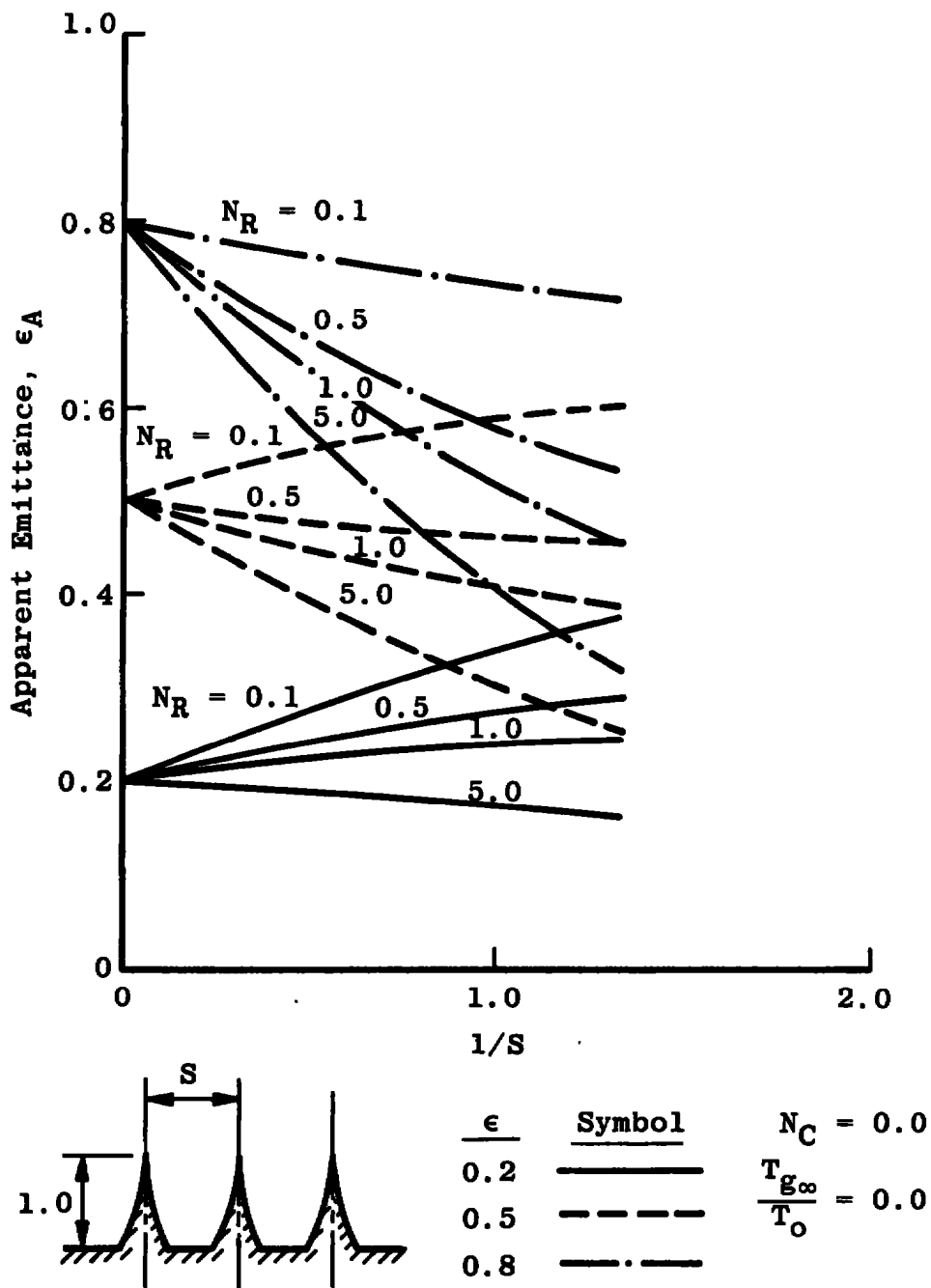


Figure 14. The apparent emittance of an inverse parabolic fin cluster.

strongly influenced by surface emissivity. Higher values of surface emissivity are seen to generally yield the highest value of apparent emittance for any particular value of  $S$  and  $N_R$ . However, a reversal of the cavity effect, i.e.,  $\epsilon_A > \epsilon$ , for high emissivities, also noted by Reference (13) for rectangular fins, exists for the fin configurations investigated in this study. For  $\epsilon = 0.2$ ,  $\epsilon_A$  is generally greater than 0.2. However, as  $\epsilon$  increases to 0.5 and 0.8,  $\epsilon_A$ , in most cases, becomes less than  $\epsilon$ . The explanation for this trend lies in the fact that for low values of  $\epsilon$ , the base radiation is reflected from the fins and augments the radiation to the external environment, while for high values of  $\epsilon$ , the base radiation is absorbed by the fin surfaces and is reemitted at a lower temperature resulting from the conduction loss along the fin, thus, limiting the base contribution to the overall heat transfer rate.

The influence of  $N_R$  upon  $\epsilon_A$  for a fixed value of fin spacing is also apparent in Figures 12, 13, and 14. The apparent emittance is seen to decrease as  $N_R$  increases because either the amount of base radiation absorbed by the fins becomes increasingly larger or internal conduction along the fin is decreased.

A comparison of  $\epsilon_A$  for the various fin configurations is presented in Figure 15. Curves of  $\epsilon_A$  are presented for  $N_R$  values of 0.1 and 5.0, and for  $\epsilon$  values of 0.2, 0.5, and 0.8. Data from Reference (13), for a rectangular fin of

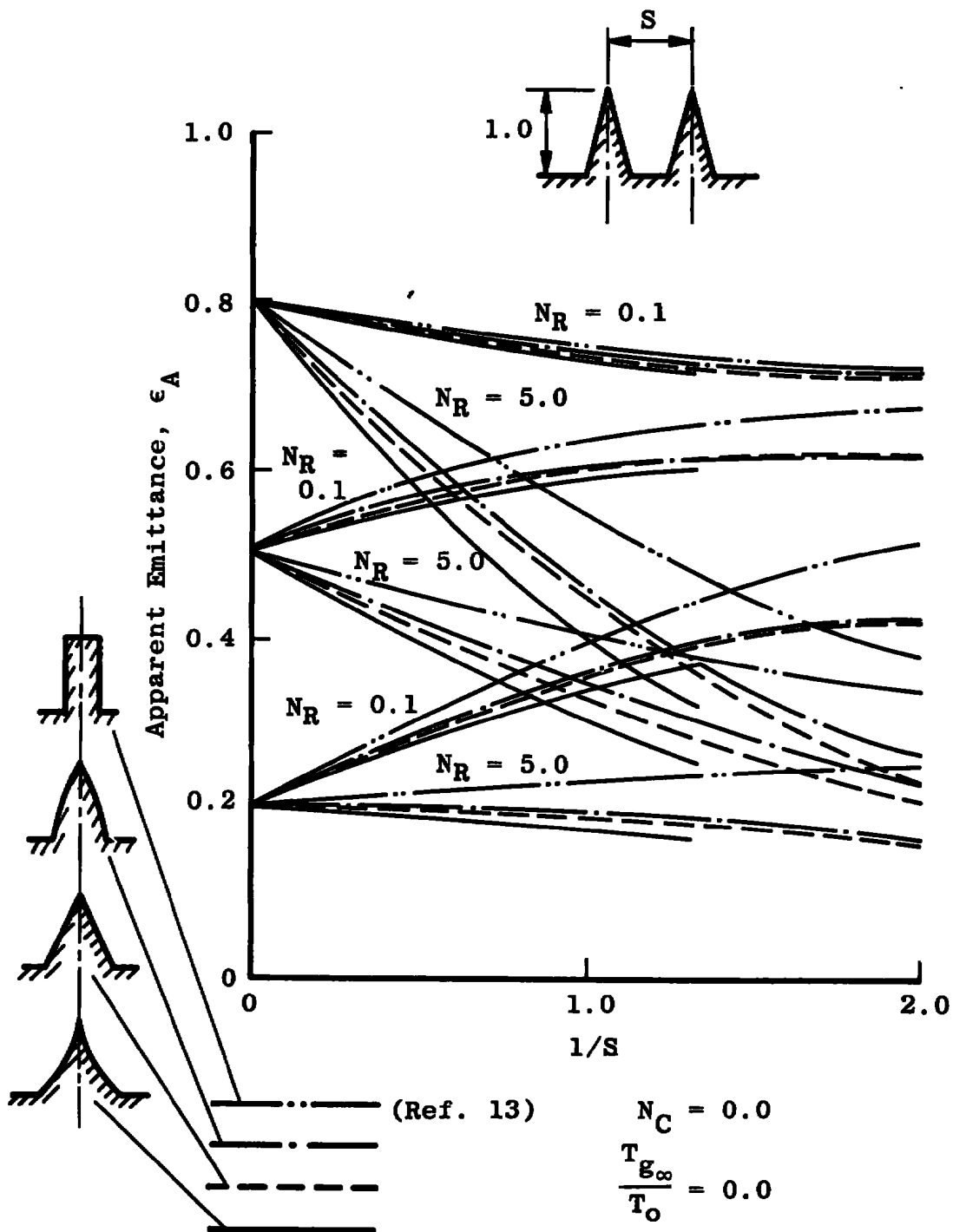


Figure 15. Apparent emittance of clusters of fins of selected shapes.

equal non-dimensional volume per unit length and fin depth, are presented for comparison purposes. Surprisingly little difference is observed between the parabolic, triangular, and inverse parabolic profiles. The rectangular fin is seen to have the highest value of  $\epsilon_A$  for any selected set of  $S$ ,  $N_R$ , and  $\epsilon$ . The data from Reference (13) for the rectangular fin have not been verified using the computer program developed for this study.

## CHAPTER VI

## CONCLUSIONS

The application, by Reference (13), of an iterative technique to the B. G. Galerkin method of treating the defining integro-differential equation constitutes a highly successful approach to the solution of this class of problems. The current extension of the method to include fins of arbitrary profile was equally successful.

Application of the method of solution shows that radiative interactions can strongly influence the temperature distribution and heat transfer characteristics of clusters of longitudinal fins.

Analysis of results indicates that only under certain circumstances can fins enhance the radiation heat transfer from the base region. For  $\epsilon \geq 0.8$  no advantage can be gained by using fins. Similarly, for  $\epsilon = 0.5$  and  $N_R \geq 0.5$  no advantages accrue from using fins, however, for  $N_R = 0.1$  an improvement in heat transfer characteristics occur when fins are used. In the case of surfaces with  $\epsilon \leq 0.2$ , fins will improve the heat transfer from the base region for all values of  $N_R \leq 1.0$ .

When conditions indicate that fins will improve the heat transfer from the base region, investigation reveals that for maximum benefit the fin spacing should be as close

as possible. This conclusion contradicts the conclusion one might draw from inspection of the fin efficiency curves, thus, illustrating why fin efficiency is not a valid parameter for fin comparisons when radiative interactions are present.

The rectangular fin profile examined by Reference (13) appears to be superior to either the parabolic, triangular or the inverse parabolic profile when compared on the basis of equal volume per unit non-dimensional depth of fin.

**BIBLIOGRAPHY**

## BIBLIOGRAPHY

1. Harper, W. B., and D. R. Brown. "Mathematical Equations for Heat Conductions in the Fins of Air-Cooled Engines," National Advisory Committee for Aeronautics Report No. 158, Washington, D. C., 1922.
2. Gardner, K. A. "Efficiency of Extended Surfaces," Transactions of the ASME, 67:621-631, August, 1945.
3. Avrami, M., and J. B. Little. "Diffusion of Heat through a Rectangular Bar and the Cooling and Insulating Effects of Fins," Journal of Applied Physics, 13:255-264, 1942.
4. Ghai, M. L. "Heat Transfer in Straight Fins," Proceedings of the General Discussion on Heat Transfer. London: Institute of Mechanical Engineers, 1951. Pp. 180-182, 203-204.
5. Eraslan, A. H., and Walter Frost. "B. G. Galerkin Method for Heat-Transfer Solution in Longitudinal Fins of Arbitrary Shape with Nonuniform Surface Coefficients," Paper presented at the AIChE-ASME Heat Transfer Conference and Exhibit, Philadelphia, Pennsylvania, April 2, 1968.
6. Lieblein, S. "Analysis of Temperature Distribution and Radiant Heat Transfer along a Rectangular Fin," National Aeronautics and Space Administration TND-196, Washington, D. C., 1959.
7. Chambers, R. L., and E. V. Somers. "Radiation Fin Efficiency for One-Dimensional Heat Flow in a Circular Fin," Transactions of the ASME Journal of Heat Transfer, 81:327-329, March, 1959.
8. Eckert, E. R. G., T. F. Irvine, Jr., and E. M. Sparrow. "Analytic Formulation for Radiating Fins with Mutual Irradiation," ARS Journal, 30:644-646, July, 1960.
9. Sparrow, E. M., T. F. Irvine, Jr., and E. R. G. Eckert. "The Effectiveness of Radiating Fins with Mutual Irradiation," The Journal of Aerospace Sciences, 28:763-772, October, 1961.

10. Herring, R. G. "Radiative Exchange between Conduction Plates with Specular Reflection," Transactions of the ASME Journal of Heat Transfer, 88:29-36, February, 1966.
11. Sparrow, E. M., and E. R. G. Eckert. "Radiant Interaction between Fin and Base Surfaces," Transactions of the ASME Journal of Heat Transfer, 84:12-18, February, 1962.
12. Sarabia, M. F. "Heat Transfer from Finned Tube Radiators," Unpublished Master's thesis, Air Force Institute of Technology, Dayton, 1964.
13. Frost, Walter, and A. H. Eraslan. "An Iterative Method for Determining the Heat Transfer from a Fin with Radiative Interaction between the Base and Adjacent Fin Surfaces," Paper presented at the AIAA third Thermophysics Conference, Los Angeles, California, June 24, 1968.
14. Cobble, M. H. "Nonlinear Heat Transfer," Journal of the Franklin Institute, 277(3):206-216, March, 1964.
15. Hung, E. M., and F. C. Appl. "Heat Transfer in Thin Fins with Temperature-Dependent Thermal Properties and Internal Heat Generation," Transactions of the ASME Journal of Heat Transfer, 89:155-162, February, 1967.
16. Frost, Walter, and A. H. Eraslan. "Solution of Heat Transfer in a Fin with Combined Convection and Radiative Interaction between the Fin and the Surrounding Surfaces," Proceedings of the 1968 Heat Transfer and Fluid Mechanics Institute, Ashley F. Emery and Creighton A. Depew, editors, Palo Alto, California: Stanford University Press, 1968. Pp. 206-220.
17. Sparrow, E. M., and R. D. Cess. Radiation Heat Transfer. Belmont, California: Brooks/Coles Publishing Company, 1966.
18. Kantorovich, L. V., and V. I. Krylov. Approximate Methods of Higher Analysis. New York: Interscience Publishers, Inc., 1958.

APPENDIXES

## APPENDIX A

NON-DIMENSIONALIZATION OF THE BASIC  
DIFFERENTIAL EQUATION

Frequently it becomes advantageous to express the solution of a differential equation in dimensionless form. There are at least two reasons for non-dimensionalizing an analysis as enumerated:

1. A study conducted under a particular set of parametric conditions can be generalized to apply to many sets of parameters by non-dimensionalizing the solution.
2. The effects on the solution of particular parametric groups can be isolated and more easily studied if the system is non-dimensionalized.

Equations 2 and 3, representing the dimensional differential equation and its associated boundary conditions respectively, are rewritten from the text and presented as Equations A-1 and A-2.

$$K(x) [Y_1(x) - Y_2(x)] \frac{d^2 T(x)}{dx^2} + \left\{ K(x) \left[ \frac{dY_1(x)}{dx} - \frac{dY_2(x)}{dx} \right] + [Y_1(x) - Y_2(x)] \frac{dK(x)}{dx} \right\} \frac{dT(x)}{dx} - \left[ h_1(x) \sqrt{1 + \left[ \frac{dY_1(x)}{dx} \right]^2} \right]$$

$$\begin{aligned}
 & + h_2(x) \sqrt{1 + \left(\frac{dy_2(x)}{dx}\right)^2} T(x) = - \left[ h_1(x) \sqrt{1 + \left(\frac{dy_1(x)}{dx}\right)^2} \right. \\
 & \cdot \left. Tg_1(x) + h_2(x) \sqrt{1 + \left(\frac{dy_2(x)}{dx}\right)^2} Tg_2(x) \right] \\
 & + q_{R1}(x) \sqrt{1 + \left(\frac{dy_1(x)}{dx}\right)^2} + q_{R2}(x) \sqrt{1 + \left(\frac{dy_2(x)}{dx}\right)^2} \quad (A-1)
 \end{aligned}$$

$$x = 0 \text{ when } T(x) = T(0) = T_0$$

$$-K(L) \frac{dT(L)}{dx} = q_R^* + h^* [T(L) - Tg(L)] \quad (A-2)$$

The dimensional variables of Equation A-1 are non-dimensionalized by introducing the following set of dimensionless variables:

$$X = \frac{x}{L} \qquad Y_1(X) = \frac{Y_1(x)}{L} \qquad Y_2(X) = \frac{Y_2(x)}{L}$$

$$\bar{K}(X) = \frac{K(x)}{K_c} \qquad \bar{h}_1(X) = \frac{h_1(x)}{h_c} \qquad \bar{h}_2(X) = \frac{h_2(x)}{h_c}$$

$$\theta(X) = \frac{T(x) - T_0}{T_{g\infty} - T_0} \qquad \theta_{g1}(X) = \frac{T_{g1}(x) - T_0}{T_{g\infty} - T_0}$$

$$\theta_{g2}(X) = \frac{T_{g2}(x) - T_0}{T_{g\infty} - T_0} \qquad \bar{h}^*(1) = \frac{h^*(L)}{h_c}$$

$$Q_{R1} = \frac{q_{R1} L}{K_c (T_0 - T_{g\infty})} \qquad Q_{R2} = \frac{q_{R2} L}{K_c (T_0 - T_{g\infty})} \quad (A-3)$$

Performing some initial manipulation of variables in the differential terms gives the following results:

$$T(x) = (T_{g\infty} - T_o) \theta(X) + T_o$$

$$\frac{dT(x)}{dx} = \frac{d[(T_{g\infty} - T_o) \theta(X) + T_o]}{dX} \frac{dX}{dx}$$

but

$$\frac{dX}{dx} = \frac{1}{L}$$

hence

$$\frac{dT(x)}{dx} = \frac{(T_{g\infty} - T_o)}{L} \frac{d\theta(x)}{dX}$$

$$\frac{d^2T(x)}{dx^2} = \frac{d\left[\frac{(T_{g\infty} - T_o)}{L} \frac{d\theta(x)}{dX}\right]}{dX} \frac{dX}{dx} = \frac{(T_{g\infty} - T_o)}{L^2} \frac{d^2\theta(x)}{dX^2}$$

Substitution of the non-dimensionalized differential terms together with the terms of Equation A-3 into Equation A-1 yields:

$$\bar{K}(x)K_c[Y_1(x) - Y_2(x)]L \frac{(T_{g\infty} - T_o)}{L^2} \frac{d^2\theta(x)}{dX^2}$$

$$\begin{aligned}
 & + K_c \left\{ \bar{k}(x) \left[ \frac{dy_1(x)}{dx} - \frac{dy_2(x)}{dx} \right] + L \left( y_1(x) - y_2(x) \right) \frac{d\bar{k}(x)}{Ldx} \right\} \\
 & \cdot \frac{(T_{g\infty} - T_o)}{L} \frac{d\theta(x)}{dx} - h_c \left[ \bar{h}_1(x) \sqrt{1 + \left( \frac{dy_1(x)}{dx} \right)^2} \right. \\
 & \left. + \bar{h}_2(x) \sqrt{1 + \left( \frac{dy_2(x)}{dx} \right)^2} \right] \left[ (T_{g\infty} - T_o)\theta(x) + T_o \right] \\
 & = - \left[ h_c \bar{h}_1(x) \sqrt{1 + \left( \frac{dy_1(x)}{dx} \right)^2} \left\{ (T_{g\infty} - T_o)\theta_{g1}(x) + T_o \right\} \right. \\
 & \left. + h_c \bar{h}_2(x) \sqrt{1 + \left( \frac{dy_2(x)}{dx} \right)^2} \left\{ (T_{g\infty} - T_o)\theta_{g2}(x) + T_o \right\} \right] \\
 & - \frac{Q_{R1}(x)K_c(T_{g\infty} - T_o)}{L} \sqrt{1 + \left( \frac{dy_1(x)}{dx} \right)^2} \\
 & - \frac{Q_{R2}(x)K_c(T_{g\infty} - T_o)}{L} \sqrt{1 + \left( \frac{dy_1(x)}{dx} \right)^2} \tag{A-4}
 \end{aligned}$$

Factoring out the constant terms that were introduced in the non-dimensionalization process gives the following equation:

$$\begin{aligned}
 & \frac{K_c(T_{g\infty} - T_o)}{L} \left[ \bar{k}(x) \left( y_1(x) - y_2(x) \right) \frac{d^2\theta(x)}{dx^2} \right. \\
 & \left. + \left\{ \bar{k}(x) \left( \frac{dy_1(x)}{dx} - \frac{dy_2(x)}{dx} \right) + \left( y_1(x) - y_2(x) \right) \frac{d\bar{k}(x)}{dx} \right\} \frac{d\theta(x)}{dx} \right]
 \end{aligned}$$

$$\begin{aligned}
& - h_c (T_{g\infty} - T_o) \left[ \bar{h}_1(x) \sqrt{1 + \left( \frac{dy_1(x)}{dx} \right)^2} \right. \\
& + \bar{h}_2(x) \sqrt{1 + \left( \frac{dy_2(x)}{dx} \right)^2} \left. \right] \theta(x) = h_c \left[ \bar{h}_1(x) \sqrt{1 + \left( \frac{dy_1(x)}{dx} \right)^2} \right. \\
& + \bar{h}_2(x) \sqrt{1 + \left( \frac{dy_2(x)}{dx} \right)^2} \left. \right] T_o - h_c (T_{g\infty} - T_o) \\
& \left[ \bar{h}_1(x) \sqrt{1 + \left( \frac{dy_1(x)}{dx} \right)^2} \theta_{g_1(x)} + \bar{h}_2(x) \sqrt{1 + \left( \frac{dy_2(x)}{dx} \right)^2} \right. \\
& \cdot \theta_{g_2(x)} \left. \right] - h_c \left[ \bar{h}_1(x) \sqrt{1 + \left( \frac{dy_1(x)}{dx} \right)^2} \right. \\
& + \bar{h}_2(x) \sqrt{1 + \left( \frac{dy_2(x)}{dx} \right)^2} \left. \right] T_o - \frac{K_c (T_{g\infty} - T_o)}{L} \\
& \left[ Q_{R1} \sqrt{1 + \left( \frac{dy_1(x)}{dx} \right)^2} + Q_{R2} \sqrt{1 + \left( \frac{dy_2(x)}{dx} \right)^2} \right] \quad (A-5)
\end{aligned}$$

Next by dividing Equation A-5 through by the factored constant group  $K_c (T_{g\infty} - T_o) / L$ , the following transformed equation is derived:

$$\begin{aligned}
& \bar{K}(x) [Y_1(x) - Y_2(x)] \frac{d^2\theta(x)}{dx^2} + \left\{ \bar{K}(x) \left[ \frac{dy_1(x)}{dx} - \frac{dy_2(x)}{dx} \right] \right. \\
& + [Y_1(x) - Y_2(x)] \left. \frac{d\bar{K}(x)}{dx} \right\} \frac{d\theta(x)}{dx}
\end{aligned}$$

$$\begin{aligned}
& - \frac{Lh}{K_c} \left[ \bar{h}_1(x) \sqrt{1 + \left( \frac{dy_1(x)}{dx} \right)^2} + \bar{h}_2(x) \sqrt{1 + \left( \frac{dy_2(x)}{dx} \right)^2} \right] \theta(x) \\
& = - \left\{ \frac{h_c L}{K_c} \left[ \bar{h}_1(x) \sqrt{1 + \left( \frac{dy_1(x)}{dx} \right)^2} \theta g_1(x) \right. \right. \\
& \quad \left. \left. + \bar{h}_2(x) \sqrt{1 + \left( \frac{dy_2(x)}{dx} \right)^2} \theta g_2(x) \right] + Q_{R1} \sqrt{1 + \left( \frac{dy_1(x)}{dx} \right)^2} \right. \\
& \quad \left. + Q_{R2} \sqrt{1 + \left( \frac{dy_2(x)}{dx} \right)^2} \right\} \quad (A-6)
\end{aligned}$$

Equation A-6 is the non-dimensional form of the general differential equation and is written in the text as Equation 15.

The first boundary condition is non-dimensionalized by a simple substitution of the dimensionless variables into Equation A-2. Equation A-7 is the non-dimensional expression for the first boundary condition.

$$\text{At } X = 0, \theta(0) = \frac{T(0) - T_o}{T_{g\infty} - T_o} = \frac{T_o - T_o}{T_{g\infty} - T_o} = 0 \quad (A-7)$$

Upon substitution of the dimensionless variables into the second boundary condition, the following relationship is produced:

$$- \bar{K}(1) K_c \frac{d[(T_{g\infty} - T_o)\theta(1) + T_o]}{dx} \frac{dx}{dx} = \frac{K_c (T_{g\infty} - T_o)}{L} Q_R^*$$

$$\begin{aligned}
& + h_c \bar{h}^*(1) \{ (T_{g\infty} - T_o) \theta(1) + T_o \} \\
& - \{ (T_{g\infty} - T_o) \bar{\theta}_g(1) + T_o \} \\
& - \frac{\bar{K}(1) K_c}{L} (T_{g\infty} - T_o) \frac{d\theta(1)}{dx} = \frac{K_c (T_{g\infty} - T_o)}{L} Q_R^* \\
& + h_c \bar{h}^*(1) \{ (T_{g\infty} - T_o) (\theta(1) - \bar{\theta}_g(1)) \} \\
\frac{d\theta(1)}{dx} + \frac{h_c \bar{h}^*(1) L}{\bar{K}(1) K_c} \theta(1) & = \frac{h_c \bar{h}^*(1) L}{\bar{K}(1) K_c} \bar{\theta}_g(1) - \frac{Q_R^*}{\bar{K}(1)}
\end{aligned}$$

Now by letting  $\beta^* = h_c \bar{h}^*(1) L / K(1) K_c$ , the second boundary condition takes on its final dimensionless form:

$$\frac{d\theta(1)}{dx} + \beta^* \theta(1) = \beta^* \bar{\theta}_g(1) - \frac{Q_R^*}{\bar{K}(1)} \tag{A-8}$$

Equations A-7 and A-8 are represented as Equation 15 in the text.

## APPENDIX B

BOUNDARY CONDITION CHECK OF ASSUMED  
GALERKIN FUNCTIONS

It is demonstrated, in the text, how the assumed form of the B. G. Galerkin functions are applied in obtaining a solution of the differential equation. It remains to show that the assumed form of the solution does satisfy the boundary conditions.

The assumed solution and the boundary conditions are rewritten from the text and stated here as Equations B-1 and B-2 respectively.

Assumed Solution:

$$\psi(x) = a_1 \phi_1(x) + \sum_{i=2}^n a_i \phi_i(x) \quad (B-1)$$

Boundary Conditions:

$$1. \quad \psi(0) = 0 \text{ at } x = 0$$

$$2. \quad \frac{d\psi(1)}{dx} + \beta^* \psi(1) = 0 \text{ at } x = 1 \quad (B-2)$$

The assumed form of the Galerkin functions is repeated here in Equation B-3.

$$\phi_1(x) = (x - \gamma^*) x^2$$

$$\gamma^* = (3 + \beta^*) / (2 + \beta^*)$$

$$\phi_i(x) = (1 - x)^2 x^{i-1} \quad (\text{B-3})$$

Substitution of the assumed solution into the first boundary condition gives:

$$\psi(0) = a_1(0 - \gamma^*) (0)^2 + \sum_{i=2}^n a_i (1 - 0)^2 (0)^{i-1} = 0 \quad (\text{B-4})$$

Next, substitution of the assumed solution into the second boundary condition gives:

$$\begin{aligned} \frac{d\psi(1)}{dx} + \beta^* \psi(1) &= \frac{d \left[ a_1 \phi_1(1) + \sum_{i=2}^n a_i \phi_i(1) \right]}{dx} \\ &+ \beta^* [a_1 \phi_1(1) + \sum_{i=2}^n a_i \phi_i(1)] \\ &= a_1 [3(1)^2 - 2(1)\gamma^*] \\ &+ \sum_{i=2}^n a_i [(i+1)(1)^i - 2i(1)^{i-1} + (i-1)(1)^{i-2}] \\ &+ \beta^* \{ a_1 [(1)^3 - (1)^2 \gamma^*] + \sum_{i=2}^n a_i [(1)^{i+1} - 2(1)^i + (1)^{i-1}] \} \\ &= a_1 [3 - 2\gamma^*] + \beta^* [a_1 (1 - \gamma^*)] \end{aligned}$$

$$\begin{aligned}
&= a_1 \left( 3 - 2 \left( \frac{3 + \beta^*}{2 + \beta^*} \right) + \beta^* \right) a_1 \left( 1 - \left( \frac{3 + \beta^*}{2 + \beta^*} \right) \right) \\
&= \frac{a_1}{(2 + \beta^*)} [6 + 3\beta^* - 6 - 2\beta^* + \beta^*(2 + \beta^* - 3 - \beta^*)] = 0
\end{aligned}$$

(B-5)

Thus it is shown how the assumed form of the Galerkin functions satisfy the boundary conditions.

## APPENDIX C

## COMPUTER PROGRAM LISTING

```

C   GENERAL SOLUTION FOR RADIATION CONVECTION FIN
      IMPLICIT REAL*8(A-H,O-Z)
      DIMENSION Z(30,30),ZH(30),ZH2(30),COLUMN(30),SA(30),CHI(60,60),
      1CAPLAM(60,60),QUEDOT(50),      OLAST(50),CAPPSI(30),
      2DIFF(50),EX(30),THETA(30),A(30),ZH1(30),SHAPE(60,60),TRAT(30),
      3TEMPAV(50)
      DIMENSION F2X(51),F1X(51),FOX(51),GX(51)
      SQRT(0)=DSQRT(0)
      ABS(0)=DABS(0)
      Y1X(X)=.3*(1.-X)**2
      Y2X(X)=-.3*(1.-X)**2
      DY1DX(X)=-.6*(1.-X)
      DY2DX(X)= .6*(1.-X)
      H1X(X)=1.+X-X
      H2X(X)=1.+X-X
      SY1(DX1)=1.+(DX1*DX1)
      SY2(DX2)=1.+(DX2*DX2)
      F2X1(Y1,Y2)=AKX*(Y1-Y2)*AR
      F1X1(Y1,Y2,DX1,DX2)=(DKDX*(Y1-Y2)+AKX*(DX1-DX2))*AR
      FOX(H1,H2,S1,S2)=8*((H1*(S1**0.5))+(H2*(S2**0.5)))*AR
      GX1(H1,H2,S1,S2)=B*((H1*TG1X*(S1**0.5))+(H2*TG2X*(S2**0.5)))*AR
      EPS2(X)=EFIN+X-X
      EPS1(X)=EFIN+X-X
      R=0.0
      WRITE(6,1110)
1110  FORMAT(' INVERSE PARABOLIC FIN WITH SLOPE INCLUDED. ')
      WRITE(6,1120)
1120  FORMAT(' UNIFORM FILM COEFFICIENT ,H1X=H2X=1.0 ')
C   DEFINE FIN FUNCTIONS
      AR=0.04/3.
      AKX=1.
      AKO=AKX
      AKC=AKO
      DKDX=0.
      TG1X=1.
      TG2X=1.
C   EVALUATION OF FIN FUNCTIONS AT X=0.
      X=.00000001
      DAO=Y1X(X)-Y2X(X)
      F2X(1)=F2X1(Y1X(X),Y2X(X))*0.5

```

```

F1X(1)=F1X1(Y1X(X),Y2X(X),DY1DX(X),DY2DX(X))*0.5
FOX(1)=FOX1(H1X(X),H2X(X),SY1(DY1DX(X)),SY2(DY2DX(X)))*0.5
GX(1)=GX1(H1X(X),H2X(X),SY1(DY1DX(X)),SY2(DY2DX(X)))*0.5
C   END X=0.
C   EVALUATION OF FIN FUNCTIONS AT X=1.
C   EVALUATION OF TIP PARAMETERS
X=.99999999
DAS=Y1X(X)-Y2X(X)
HS=0.5*(H1X(X)+H2X(X))
BS=(HS/AKX)*B
TGS=0.5*(TG1X+TG2X)
GMS=(3.+BS)/(2.+BS)
F2X(51)=F2X1(Y1X(X),Y2X(X))*0.5
F1X(51)=F1X1(Y1X(X),Y2X(X),DY1DX(X),DY2DX(X))*0.5
FOX(51)=FOX1(H1X(X),H2X(X),SY1(DY1DX(X)),SY2(DY2DX(X)))*0.5
GX(51)=GX1(H1X(X),H2X(X),SY1(DY1DX(X)),SY2(DY2DX(X)))*0.5
C   END X=1.
C   END DEFINITION OF TIP PARAMETERS
SX=-1.
DO 1030 IX=2,50
SX=-SX
AX=1.+0.5*(1.+SX)
XI=IX-1
X=0.02*XI
F2X(IX)=F2X1(Y1X(X),Y2X(X))*AX
F1X(IX)=F1X1(Y1X(X),Y2X(X),DY1DX(X),DY2DX(X))*AX
FOX(IX)=FOX1(H1X(X),H2X(X),SY1(DY1DX(X)),SY2(DY2DX(X)))*AX
GX(IX)=GX1(H1X(X),H2X(X),SY1(DY1DX(X)),SY2(DY2DX(X)))*AX
1030 CONTINUE
C   END FUNCTION STORAGE
C   MAXIMUM MATRIX DIMENSIONS, NC=20, ND=21
C   START LOOP FOR EVALUATION OF MATRIX ELEMENTS
NR=1
NC=20
ND=NR+NC
SI211=0.
SI111=0.
SI011=0.
SJ01=0.
SJ11=0.
SJ21=0.
SSHF=0.
SJS1=0.

```

```

C      START NUMERICAL INTEGRATION FOR (1,1) AND (1,ND)
      DO1031 IX=1,51
      XI=IX-1
      X=0.02*XI
      P11X=X**X-X-GMS*X*X
      TI211=(F2X(IX))*(6.*X-2.*GMS)*P11X
      TI111=(F1X(IX))*(3.*X-2.*GMS*X)*P11X
      TIO11=(FOX(IX))*(X**X-GMS*X*X)*P11X
      TJO1=(FOX(IX))*(X*X-X)*P11X
      TJ11=(F1X(IX))*(2.*X-1.)*P11X
      TJ21=(F2X(IX))*P11X
      TJS1=(GX(IX))*P11X
      TSHF=GX(IX)
      SI211=SI211+TI211
      SI111=SI111+TI111
      SIO11=SI011+TIO11
      SJO1=SJO1+TJO1
      SJ11=SJ11+TJ11
      SJ21=SJ21+TJ21
      SJS1=SJS1+TJS1
      SSHF=SSHF+TSHF
1031 CONTINUE
C      END INTEGRATION FOR (1,1) AND (1,ND)
      Z(1,1)=SI211+SI111-SIO11
      ZH(1)=RS*TGS*(SJO1-SJ11-2.*SJ21)-SJS1
      ZH1(1)=(SJO1 - SJ11- 2.* SJ21 )
      SHF=SSHF
      DO5000 I=2,NC
      ZI=I
      SI21I=0.
      SI11I=0.
      SIO1I=0.
C      START NUMERICAL INTEGRATION FOR (1,I)
      DO1032 IX=1,51
      XI=IX-1
      X=0.02*XI
      P1IX=X-GMS
      TI21I=(F2X(IX))*(((ZI-1.)*(ZI-2.)*(X**(I-1)))-((2.*ZI)*(ZI-1.)*(X
1**I))+((ZI+1.)*(ZI)*(X**(I+1))))*P1IX
      TI11I=(F1X(IX))*(((ZI-1.)*(X**I))-((2.*ZI)*(X**(I+1)))+(ZI+1.)*(
1X**(I+2))))*P1IX
      TIO1I=(FOX(IX))*((X**(I+1))-(2.*(X**(I+2)))+(X**(I+3)))*P1IX
      SI21I=SI21I+TI21I

```

```

      S1111=S1111+T1111
      S1011=S1011+T1011
1032 CONTINUE
C     END INTEGRATION FOR (1,1)
      Z(1,1)=S1211+S1111-S1011
5000 CONTINUE
      DO5010 K=2,NC
      7K=K,
      S12K1=0.
      S11K1=0.
      S10K1=0.
      SJ0K=0.
      SJ1K=0.
      SJ2K=0.
      SJSK=0.
C     START NUMERICAL INTEGRATION FOR (K,1) AND (K,ND)
      DO1033 IX=1,51
      XI=IX-1
      X=0.02*XI
      PK1X=(X**(K-1))-(2.*(X**K))+(X**(K+1))
      T12K1=(F2X(IX))*(6.*X-2.*GMS)*PK1X
      T11K1=(F1X(IX))*(3.*X*X-2.*GMS*X)*PK1X
      T10K1=(FOX(IX))*(X**3-GMS*X*X)*PK1X
      TJ0K=(FOX(IX))*(X*X-X)*PK1X
      TJ1K=(F1X(IX))*(2.*X-1.)*PK1X
      TJ2K=(F2X(IX))*PK1X
      TJSK=(GX(IX))*PK1X
      S12K1=S12K1+T12K1
      S11K1=S11K1+T11K1
      S10K1=S10K1+T10K1
      SJ0K=SJ0K+TJ0K
      SJ1K=SJ1K+TJ1K
      SJ2K=SJ2K+TJ2K
      SJSK=SJSK+TJSK
1033 CONTINUE
C     END INTEGRATION FOR (K,1) AND (K,ND)
      Z(K,1)=S12K1+S11K1-S10K1
      ZH(K)=BS*TGS*(SJ0K-SJ1K-2.*SJ2K)-SJSK
      ZH1(K)=(SJ0K-SJ1K-2.*SJ2K)
5010 CONTINUE
      DO5020 K=2,NC
      ZK=K
      DO5030 I=2,NC

```

```

      ZI=I
      SI2KI=0.
      SI1KI=0.
      SIOKI=0.
C     START NUMERICAL INTEGRATION FOR (K,I)
      DO1034 IX=2,51
      XI=IX-1
      X=0.02*XI
C     IX STARTS AT 2 SINCE FOR IX=1 X=0 AND THUS PKIX=0
      PKIX= ((1.-X)*(1.-X)*X**([I+K-4]))
      T12KI=(F2X(IX))*(((ZI-1.)*(ZI-2.))-((2.*ZI)*(ZI-1.)*X)+((ZI+1.)*ZI
1 *X*X))*PKIX
      T11KI=(F1X(IX))*((ZI-1.)-(2.*ZI*X)+((ZI+1.)*X*X))*X*PKIX
      T10KI=(FOX(IX))*(1.-X)*(1.-X)*X*X*PKIX
      SI2KI=SI2KI+T12KI
      SI1KI=SI1KI+T11KI
      SIOKI=SIOKI+T10KI
1034 CONTINUE
C     END INTEGRATION FOR (K,I)
      Z(K,I)=SI2KI+SI1KI-SIOKI
      5030 CONTINUE
      5020 CONTINUE
C     END EVALUATION OF MATRIX ELEMENTS
C*****
C*****
C     THE FOLLOWING ARE CERTAIN INDEXING CONSTANTS AND SOME INITIAL VALUES
      I=20
C     I REPRESENTS THE NUMBER OF ELEMENTS THE FIN IS DIVIDED INTO FOR RAD.INTEG.
      K=I
C     N REPRESENTS THE ORDER OF THE GALERKIN ASSUMPTION ON THE SOLUTION
      N=10
C     IB REPRESENTS THE NUMBER OF ELEMENTS INTO WHICH THE BASE IS DIVIDED
      IB=5
      I2 =I+1
      I3 =2*I
      I4=I3+1
      I5=I3+IB
      I6=I5+1
C     IEND CORRESPONDS TO THE TOTAL ELEMENT NO.AND INCLUDES BASE
      IEND=I5
      JSTOP=I6
      THETA(K)=0.0
      QSTAR =0.0

```

```

      TRATC=0.0
      EPSGAS=.9999
C*****
C*****
C*****
C THE FOLLOWING IS A SEARCH FOR THE SMALLEST ELEMENT OF THE Z MATRIX
      AMIN=1.0
      DO 350 IY=1,N
      DO 350 KY=1,N
      AA=DABS(Z(IY,KY))-DABS(AMIN)
      IF (AA) 351,351,350
      351 AMIN=DABS(Z(IY,KY))
      350 CONTINUE
C*****
C*****
C THE FOLLOWING IS A NORMALIZATION OF THE Z MATRIX BY DIVISION BY THE MIN ELEM.
C THE MINIMUM ELEMENT IS CALLED AMIN
      DO 180 N1=1,N
      DO 180 N2=1,N
      Z(N1,N2) =Z(N1,N2)/AMIN
      180 CONTINUE
C *****
C CALLING THE REVISED DOUBLE PRECISION INVERSION ROUTINE"VERTDR"
      CALL VERTDR (N,30,Z,ICHECK)
C*****
      DO 181 N3=1,N
      DO 181 N4=1,N
      Z(N3,N4)=Z(N3,N4)/AMIN
      181 CONTINUE
C*****
      IF (ICHECK +1) 133,134,133
      134 WRITE (6,610)
      610 FORMAT(' Z(K,I) MATRIX IS SINGULAR - SORRY ABOUT THAT CHIEF')
      133 CONTINUE
C *****
C*****
C*****
      EFIN=.2
C INSERT DO HERE FOR PERMUTATION ON FIN EMISSIVITY
      BASE=1.
C INSERT DO HERE FOR PERMUTATION ON FIN SPACING
C BASE IS THE NONDIMENSIONAL FIN PITCH
C ALONG IS THE RATIO OF NON-DIM.FIN LENGTHIN SUBROUTINE FACTOR TO THE NON-

```

```

C DIMENSIONAL FIN LENGTH IN THE MAIN PROGRAM.
  ALONG=1./(BASE-.6)
C BASE1 IS THE BASE WIDTH OF THE UPPER FIN SURFACE.
  BASE1= .3*ALONG
C BASE2 IS THE BASE WIDTH OF THE LOWER FIN SURFACE.
  BASE2= .3*ALONG
C*****
C*****
C*****
C THE FOLLOWING SECTION TAKES THE SHAPE FACTOR MATRIX 'SHAPE' FROM
C SUBROUTINE FACTOR AND COMPUTES THE 'CHI' MATRIX
  CALL FACTOR (SHAPE ,I,IB,BASE1,BASE2,ALONG)
C CALCULATION OF THE 'CHI' MATRIX ELEMENTS FOLLOWS
  DO 171 JL=1,16
    DO 160 IL=1,I
      CI=I
      CIL=IL
      EPSI1= EPS1((2.*CIL-1.)*(1./(2.*CI)))
      IF (IL-JL) 161,162,161
161 CHI(IL,JL)= -(1.-EPSI1)/EPSI1)* SHAPE(IL,JL)
      GO TO 160
162 CHI(IL,JL) = (1.-((1.-EPSI1)*SHAPE(IL,JL)))/EPSI1
160 CONTINUE
      DO 163 IL=12,I3
        EPSI2= EPS2((2.*(CIL-CI)-1.)*(1./(2.*CI)))
        IF (IL-JL) 164,165,164
164 CHI(IL,JL) = -(1.-EPSI2)/EPSI2)*SHAPE(IL,JL)
        GO TO 163
165 CHI(IL,JL) = (1.-((1.-EPSI2)*SHAPE(IL,JL)))/EPSI2
163 CONTINUE
      DO 166 IL= 14,I5
        EPS3=EFIN
        EPSI3= EPS3
        IF (IL-JL) 167,168,167
167 CHI(IL,JL) = -(1.-EPSI3)/EPSI3)*SHAPE(IL,JL)
        GO TO 166
168 CHI(IL,JL) = (1.-((1.-EPSI3)* SHAPE(IL,JL)))/EPSI3
166 CONTINUE
      IF (I6-JL) 169,170,169
169 CHI(I6,JL) = -(1.-EPGAS)/EPGAS)* SHAPE(I6,JL)
        GO TO 171
170 CHI(I6,JL) = (1.-((1.-EPGAS)*SHAPE(I6,JL)))/EPGAS
171 CONTINUE

```

```

C CALLING SUBROUTINE VERTD
      CALL VERTD (I6,60,CHI,JCHECK)
      IF (JCHECK+1) 172,173,172
173 WRITE(6,630)
630 FORMAT (' THE CHI MATRIX IS SINGULAR. THE PROGRAM WILL CONTINUE')
172 CONTINUE
C*****
C*****
C EVALUATION OF THE CAP LAMBDA FUNCTIONS USING THE CHI MATRIX
      DO 100 M=1,JSTOP
C THE SUBSCRIPT M IS EQUIVALENT TO THE SUBSCRIPT I IN THE ANALYSIS
      CM=M
      IF (M-1) 103,103,101
101 IF (M-13) 104,104,102
102 IF (M-15) 105,105,106
103 EPS = EPS1((CM-.5)/CI)
      GO TO 107
104 EPS = EPS2(((CM-CI)-.5)/CI)
      GO TO 107
105 EPS = EPS3
      GO TO 107
106 EPS = EPSGAS
107 EPSCON = EPS/(1.-EPS)
      DO 100 MM=1,JSTOP
C THE SUBSCRIPT MM IS EQUIVALENT TO THE SUBSCRIPT K IN THE ANALYSIS
      CN=MM
      IF (M-MM) 1008,109,1008
1008 CAPLAM(M,MM)= EPSCON * (-CHI(M,MM))
      GO TO 100
109 CAPLAM(M,MM)= EPSCON * (1.-CHI(M,MM))
100 CONTINUE
C*****
C INSERT DO HERE FOR PERMUTATION ON RADIATION NUMBER (RN).
      RN=-5.
C*****
      ICOUNT = 0
C*****
      DO 108 M=1,JSTOP
      QUEDNT(M)=0.0
      TEMPAV(M)=0.0
108 CONTINUE
C*****
      GO TO 150

```

```

2000 CONTINUE
      DO 1001 M=1,JSTOP
      SUM=0.0
      DO 1101 MM= 1,I
      SUM=SUM+CAPLAM(M,MM)*((1.+((TRATC)-1.0)*THETA(MM))**4)
1101 CONTINUE
      DO 1102 MM= I2,I3
      SUM=SUM+CAPLAM(M,MM)*((1.+((TRATC)-1.0)*THETA(MM-I))**4)
1102 CONTINUE
      DO 1103 MM=I4,I5
      SUM=SUM+CAPLAM(M,MM)
1103 CONTINUE
      SUM=SUM+CAPLAM(M,I6)*(TRATC**4)
      QUEDOT(M)= RN*SUM
      DIFF(M)= QUEDOT(M)- QLAST(M)
1001 CONTINUE
C PROGRAM LOGIC FOR CHECKING ON CONVERGENCE OF ITERATIVE METHOD FOLLOWS
      ILOOK =0
151 ILOOK = ILOOK + 1
      IF (ILOOK - I3) 152,152,1540
152 IF(DABS(DIFF(ILOOK))-DABS(QUEDOT(ILOOK)*.001))151,151,153
153 CONTINUE
      OSTAR =RN* ( (EPS1(1.)+EPS2(1.))/2.)* (((THETA(K)* (TRATC-1.0)
      1+1.)**4)-(TRATC)**4)
C*****
150 CONTINUE
C*****
C NUMERICAL INTEGRATION TO EVALUATE ZH2(1)
      CONST = (1./CI)/3.
      Y1N=((QUEDOT(I)-QUEDOT(I-1)-QUEDOT(I))/2.)*((1.+DY1DX(1.))**2)**
      1.5)+(QUEDOT(I3)+(QUEDOT(I3)-QUEDOT(I3-1))/2.)*((1.+DY2DX(1.))**2)
      2)**.5)**(1.-GMS)
      EVEN=0.0
      ODD=0.0
      ISTOP = I-2
      NC=N
      DO 120 KK =2,ISTOP,2
      CCK=KK
      EVEN = EVEN+ (((QUEDOT(KK)+QUEDOT(KK+1))/2.)*((1.+ DY1DX(CCK/CI)**
      12)**.5)+((QUEDOT(KK+I)+QUEDOT(KK+I+1))/2.) * ((1.+ DY2DX(CCK/CI)**
      22)**.5)) * ((CCK/CI)**3.)-GMS*((CCK/CI)**2))
      CCKO=CCK+1.
      ODD = ODD + ((( QUEDOT (KK+1)+ QUEDOT(KK+2))/2.)*((1.+DY1DX(CCKO/C

```

```

11)**2)**.5)+(QUEDOT(KK+1+I)+QUEDOT(KK+I+2))/2.)*(1.+DY2DX(CKK0/C
21)**2)**.5))*(((CCK0/CI)**3)-GMS*((CCK0/CI)**2))
120 CONTINUE
  Y11=(((QUEDOT(1)+QUEDOT(2))/2.)*(1.+DY1DX(1./CI)**2)**.5)+((
1QUEDOT(1+1)+QUEDOT(1+2))/2.)*(1.+DY2DX(1./CI)**2)**.5))*
2( (1./CI)**3.0- GMS*((1./CI)**2))
C APPLICATION OF SIMPSONS RULE GIVES FOR ZH2(1) THE FOLLOWING
ZH2(1) = CONST *(4.*(Y11+ ODD)+2.*EVEN + Y1N)
C NUMERICAL INTEGRATION TO EVALUATE ZH2(K) K= 2,N
DO 121 KEXP=2,NC
C YK(ZERO)AND Y<(N) = ZERO
  ODD= 0.0
  EVEN= 0.0
  DO 122 KK= 2,ISTOP,2
    CCK=KK
    D=CCK/CI
    CCK0=CCK+1.
    ODD=CCK0/CI
    AKEXP = KEXP
    EVEN = EVFN +(((QUEDOT(KK)+ QUEDOT(KK+1))/2.)*(1.+ DY1DX(D)
1**2)**.5)+((QUEDOT(KK+I)+ QUEDOT(KK+1+I))/2.)*(1.+DY2DX(D)
2**2)**.5))*((DD*(AKEXP+1.)-2.*(DD*(AKEXP))+DD*(AKEXP-1.)))
    ODD = ODD +(((QUEDOT(KK+1)+ QUEDOT(KK+2))/2.)*(1.+DY1DX(DD)**2)
1**2)**.5)+ (( QUEDOT (KK+1+I) + QUEDOT(KK +I+2))/2.)*(1.+DY2DX(DD)**2
2)**2)**.5))*((DD*(AKEXP+1.)-2.*(DD*(AKEXP))+DD*(AKEXP-1.))
122 CONTINUE
  YK1=(((QUEDOT(1)+QUEDOT(2))/2.)*(1.+DY1DX(1./CI)**2)**.5)+
1((QUEDOT(1+1)+QUEDOT(1+2))/2.)*(1.+DY2DX(1./CI)**2)**.5))*
2((1./CI)**(AKEXP+1.)-2.*((1./CI)**AKEXP)+(1./CI)**(AKEXP-1.))
C APPLICATION OF SIMPSONS RULE GIVES FOR ZH2(K) THE FOLLOWING
ZH2(KEXP)= CONST* (4.*(YK1+ODD)+2.*EVEN)
121 CONTINUE
C EVALUATION OF THE COLUMN MATRIX ELEMENTS FOLLOWS
DO 123 KK=1,NC
  COLUMN(KK)= ZH(KK) -(OSTAR*ZH1(KK))/AKX + ZH2(KK)
123 CONTINUE
C*****
C*****
C EVALUATION OF THE A(H)'S FOLLOWS
C KGO = K , IGO = I
DO 127 KGO =1,N
  A(KGO)=0.0
DO 127 IGO =1,N

```

```

      A(KGO)=A(KGO)+COLUMN(IGO)*Z(KGO,IGD)
127 CONTINUE
C*****
C*****
C      EVALUATION OF CAPPSI(MO)  MO=1,K
      CONST2 =QS* TGS - QSTAR/ AKX
      DO 129 MO=1,K
      CKK=K
      AMO=MO
      EX(MO)= (2.*AMO-1.)/(2.*CKK)
      CAPSI1 = A(1)*(EX(MO)-GMS)*(EX(MO)**2.)
      CAPPSI(MO)= CAPSI1
      DO 128 MOO =2,N
      AMOO = MOO
      CAPPSI(MO)= CAPPSI(MO)+ A(MOO)*(EX(MO)**(AMOO+1.)-2.*(EX(MO)**AMOO
1)+ EX(MO)**(AMOO-1.))
128 CONTINUE
C*****
C      EVALUATION OF THETA (I)
      THETA(MO)= CAPPSI(MO)+ CONST2 * (EX(MO)**2-EX(MO))
      TRAT(MO)=THETA(MO)*(TRATC-1.0)+1.0
129 CONTINUE
C*****
C*****
C      CHECKING FOR DIVERGENCE OF SOLUTION
      DO 1282 MA=1,K
      IF (THETA(MA)+1)1280,1280,1281
1281 IF (THETA(MA)-2.0)1282,1282,1283
1280 THETA(MA)=-1.0
      GO TO 1282
1283 THETA(MA)=2.0
1282 CONTINUE
C*****
C*****
C      AVERAGING THETA FOR THE NEXT ITERATION
      FCOUNT=ICOUNT+1
      DO 1285 NUB=1,I
      THETA(NUB)=(TEMPAV(NUB)*(FCOUNT-1.0)+THETA(NUB))/FCOUNT
      TEMPAV(NUB)=THETA(NUB)
1285 CONTINUE
C*****
C*****
C      THE NEXT COMPUTATION SAVES THE N-TH QUOTD ITERATION BEFORE GOING ON

```

```

      DO 140 I0 =1,I3
      QLAST(I0)= QUEDOT(I0)
      140 CONTINUE
C*****
C ICOUNT IS THE COUNTER FOR KEEPING TRACK OF THE NUMBER OF ITERATIONS PERFORMED
      ICOUNT = ICOUNT + 1
      IF(ICOUNT-30)2000,2000,156
C*****
      1540 WRITE(6,603) ICOUNT
      603 FORMAT ('1THE ITERATION CONVERGED ON THE ('I2')TH ITERATION. RESUL
      ITS FOLLOW.')
```

C\*\*\*\*\*  
C CALCULATION OF THE FIN PERFORMANCE PARAMETERS FOLLOWS.  
C QRSUM REPRESENTS THE ACTUAL FIN HEAT TRANSFER BY RADIATION.

```

      154 QRSUM = 0.0
      DO 190 LA =1,I
      FLA=LA
      QRSUM = QRSUM +(QUEDOT(LA)/CI)*((1.+(DY1DX((FLA-.5)/CI))**2)**.5)
      QRSUM = QRSUM +(QUEDOT(LA+I)/CI)*((1.+(DY2DX((FLA-.5)/CI))**2)**
      1.5)
      190 CONTINUE
      QRSUM = QRSUM + QSTAR * (Y1X(1.)-Y2X(1.))
C QCSUM REPRESENTS THE ACTUAL FIN HEAT TRANSFER BY CONVECTION.
      QCSUM = 0.0
      DO 191 LB=1,I
      FLB=LB
      QCSUM= QCSUM +(B/CI)*(THETA(LB)-1.)*(H1X((FLB-.5)/CI)*((1.+(DY1DX(
      1(FLB-.5)/CI))**2)**.5)+ H2X((FLB-.5)/CI)*((1.+(DY2DX((FLB-.5)/CI))
      2**2)**.5))
      191 CONTINUE
      QCSUM= QCSUM + B* (THETA(I)-1.)*((H1X(1.)+H2X(1.))/2.)*(Y1X(1.)-
      1Y2X(1.))
C QRBASE REPRESENTS THE ACTUAL BASE HEAT TRANSFER BY RADIATION
      QRBASE =0.0
      AREAR = BASE -(Y1X(0.0)-Y2X(0.0))
      DO 192 LC=14,I5
      FIR=IR
      QRBASE = QRBASE + QUEDOT(LC)* (AREAR/FIR)
      192 CONTINUE
C QCBASE REPRESENTS THE ACTUAL BASE HEAT TRANSFER BY CONVECTION.
      QCBASE =-R*((H1X(0.0)+H2X(0.0))/2.)*AREAR
C QRBID IS THE IDFAL BASE RADIATION HEAT TRANSFER.
      QRBID=RN*(1.-TRATC**4)*AREAR
```

```

C QCRID IS THE IDEAL BASE CONVECTION HEAT TRANSFER
  QCRID = QCBASE
C QRFID IS THE IDEAL FIN RADIATION HEAT TRANSFER.
  QRFID = 0.0
  DO 193 LD=1,I
  FLD=L0
  QRFID=QRFID+RN*(1.-TRATC**4)*((1.+(DY1DX((FLD-.5)/CI)**2)**5)/CI+
  1(1.+(DY2DX((FLD-.5)/CI)**2)**5)/CI)
193 CONTINUE
  QRFID=QRFID+RN*(1.-TRATC**4)*(Y1X(1.)-Y2X(1.))
C QCFID IS THE IDEAL FIN CONVECTIVE HEAT TRANSFER.
  QCFID=0.0
  DO 194 LF =1,I
  FLE =LF
  QCFID=QCFID+B*(H1X((FLE-.5)/CI)*((1.+DY1DX((FLE-.5)/CI)**2)**5)+
  1H2X((FLE-.5)/CI)*((1.+DY2DX((FLE-.5)/CI)**2)**5))*(1./CI)
194 CONTINUE
  QCFID=QCFID+B*((H1X(1.)+H2X(1.))/2.)*(Y1X(1.)-Y2X(1.))
  ETA=(ORSUM +QCSUM)/(QRFID + QCFID)
  APEMIT= (ORSUM +ORBASE -OSTAR*(Y1X(1.0)-Y2X(1.0)))/(RN*(1.+
  1TRATC**4)*BASE)
  EFLUX=(ORSUM+ORBASE+QCSUM+QCBASE)/((ORBID+QCRID)*(BASE/AREA8))
  WRITE (6,641) ORSUM ,QCSUM,ORBASE,QCBASE,QRFID,QCFID, QCRID,QCRID
641 FORMAT (// ' ACTUAL FIN RADIATIVE HEAT FLUX = 'E13.5,10X,' ACTUAL F
  1IN CONVECTIVE HEAT FLUX = 'E13.5,/, ' ACTUAL BASE RADIATIVE HEAT FL
  2UX = 'E13.5,9X,' ACTUAL BASE CONVECTIVE HEAT FLUX = 'E14.5,/, ' IDEA
  3L FIN RADIATIVE HEAT FLUX = 'E13.5,11X,' IDEAL FIN CONVECTIVE HEAT
  4 FLUX = 'E13.5,/, ' IDEAL BASE RADIATIVE HEAT FLUX = 'E13.5,10X.
  5' IDEAL BASE CONVECTIVE HEATFLUX = 'E13.5)
  WRITE(6,640) ETA,APEMIT,EFLUX
640 FORMAT(' FIN EFFICIENCY = 'E13.5,/, ' APPARENT EMITTANCE = 'E13.5
  1,/, ' EFFECTIVE HEAT FLUX = 'E13.5)
155 DO 138 IT=1,I
  NT=IT +1
  WRITE (6,604) IT ,QUEDOT(IT),IT,DIFF(IT),NT,QUEDOT(NT),NT,DIFF(NT)
604 FORMAT (' QUEDOT('I2') = 'E14.7,4X,'DIFF('I2') = 'E14.7'***** QUE
  1DOT('I2') = 'E14.7,4X,'DIFF('I2') = 'E14.7)
138 CONTINUE
  WRITE(6,48)(QUEDOT(NU),NU=14,16)
  48 FORMAT(6E20.5)
  DO 139 IA= 1,N
  WRITE(6,605)IA,A(IA)
605 FORMAT(' A('I2') = 'E14.7)

```

```

139 CONTINUE
      IHALF = I/2
      IMJ 141 IT=1,IHALF
      IS=IT+IHALF
      WRITE(6,625)IT,THETA(IT),IT,TRAT(IT),IS,THETA(IS),IS,TRAT(IS)
625  FORMAT(' THETA('I2') = 'E14.7,4X,'TRAT('I2') = 'E14.7'***** THETA(
1'I2') = 'F14.7,4X, 'TRAT('I2') = 'F14.7)
141 CONTINUE
      WRITE(6,774)R
774  FORMAT(' THE CONVECTION NUMBER='F6.2)
      WRITE(6,777)RN
777  FORMAT(' THE RADIATION NUMBER='F6.2)
      WRITE(6,779)BASE
779  FORMAT(' THE FIN PITCH TO LENGTH RATIO IS 'F6.2)
      WRITE (6,780)EFIN
780  FORMAT(' FIN SURFACE EMISSIVITY = 'F6.4)
49  CONTINUE
50  CONTINUE
51  CONTINUE
      GO TO 135
156 WRITE (6,626)
626  FORMAT('THE ITERATION SCHEME FAILED TO CONVERGE IN 30 ATTEMPTS A
      IND HAS BEEN TERMINATED. VALUES EXISTING AT TERMINATION FOLLOW.')
```

```

135 STOP
```

```

*****
```

```

C
C
C
C
C
C
C
C
```

#### COMMENTS ON SUBROUTINES

```

*****
```

```

C
C
C
C
C
C
C
```

```

SUBROUTINE VERTDR IS AN AEDC IRM 360/50 LIBRARY SUBROUTINE MODIFIED TO RELAX
CERTAIN INTERNAL ACCURACY RESTRAINTS. VERTDR IS A DOUBLE PRECISION MATRIX
INVERSION SUBROUTINE.
```

```

*****
```

```

C
```

```
C
C
C SUBROUTINE FACTOR IS A DOUBLE PRECISION SUBROUTINE FOR CALCULATING THE
C SHAPEFACTORS OF THE VARIOUS ELEMENTS USED IN THE RADIATION ANALYSIS. FACTOR
C IS AN APPLICATION OF THE STRING POLYGON METHOD OF CALCULATING SHAPEFACTORS.
C FACTOR WAS DEVELOPED BY DR. WALTER FRIST OF THE UNIVERSITY OF TENNESSEE
C SPACE INSTITUTE AND WILL SOON BE PUBLISHED AS AN AFDC TDR.
C
*****
C
C
C SUBROUTINE VERTD IS AN AFDC IBM 360/50 LIBRARY SUBROUTINE FOR DOUBLE
C PRECISION MATRIX INVERSION.
C
*****
      END
```

DOCUMENT CONTROL DATA - R & D

(Security classification of title, body of abstract and indexing annotation must be entered when the overall report is classified)

1. ORIGINATING ACTIVITY (Corporate author) Arnold Engineering Development Center ARO, Inc., Operating Contractor Arnold Air Force Station, Tennessee	2a. REPORT SECURITY CLASSIFICATION <b>UNCLASSIFIED</b>
	2b. GROUP N/A

3. REPORT TITLE  
**THE SOLUTION OF COMBINED CONVECTION AND RADIATION HEAT TRANSFER FROM LONGITUDINAL FINS OF ARBITRARY CROSS-SECTION**

4. DESCRIPTIVE NOTES (Type of report and inclusive dates)  
May through November, 1968 - Final Report

5. AUTHOR(S) (First name, middle initial, last name)  
Percy B. Carter, Jr., ARO, Inc.

6. REPORT DATE April 1969	7a. TOTAL NO. OF PAGES 96	7b. NO. OF REFS 18
------------------------------	------------------------------	-----------------------

8a. CONTRACT OR GRANT NO. F40600-69-C-0001 b. PROJECT NO. c. d.	9a. ORIGINATOR'S REPORT NUMBER(S) AEDC-TR-69-88
	9b. OTHER REPORT NO(S) (Any other numbers that may be assigned this report) N/A

10. DISTRIBUTION STATEMENT  
This document has been approved for public release and sale; its distribution is unlimited.

11. SUPPLEMENTARY NOTES Available in DDC.	12. SPONSORING MILITARY ACTIVITY Arnold Engineering Development Center, Air Force Systems Command, Arnold Air Force Station, Tennessee
--	---

13. ABSTRACT  
The effects of combined radiative and convective heat transfer from arrays of longitudinal fins of arbitrary profile are analyzed subject to non-uniform surface emissivity and non-uniform surface film coefficients. Consideration is given to radiative interactions between adjacent fins and between fins and the base surface. Solution of the defining differential equation for fin temperature distribution is obtained through an iterative application of the B. G. Galerkin variational technique. Application of the method of solution is made to fins of parabolic, triangular, and inverse parabolic profile subject solely to the radiative mode of heat transfer. Effects in variations of the dimensionless radiation number,  $N_R$ , fin spacing,  $S$ , and fin surface emissivity,  $\epsilon$ , are investigated. Findings of the study reveal that for the pure radiative mode, fins can enhance the heat transfer between the base and the surroundings only for the case of low fin and base surface emissivity.

14. KEY WORDS	LINK A		LINK B		LINK C	
	ROLE	WT	ROLE	WT	ROLE	WT
heat transfer convection radiation fins mathematical analysis differential equations						